Design of gallinamide A analogs as potent inhibitors of cathepsin L and the parasite *Trypanosoma cruzi*

Paul D. Boudreau,[1,†] Bailey W. Miller,[1,†] Laura-Isobel McCall,[2,3] Jehad Almaliti,[1,4] Raphael Reher,[1] Ken Hirata,[2] Thu Le,[2] Jair L. Siqueira-Neto[2,3], Vivian Hook[2], William H. Gerwick[1,2,]*

[1]Center for Marine Biotechnology and Biomedicine, Scripps Institution of Oceanography, University of California, San Diego, La Jolla, California 92093, United States

[2]Skaggs School of Pharmacy and Pharmaceutical Sciences, University of California, San Diego, La Jolla, California 92093, United States

[3]Center for Discovery and Innovation in Parasitic Diseases, University of California, San Diego, La Jolla, California 92093, United States

[4]Department of Pharmaceutical Sciences, College of Pharmacy, the University of Jordan, Amman, 11942, Jordan

Supporting Information - Table of Contents

NMR Spectra – Leucine Extended Product

NMR Spectra – Benzylation and Esterification

NMR Spectra – Methylation of the Tail Dimer

NMR Spectra – Full Products

S6. ^{1}H and ^{13}C-NMR spectra of *tert*-butyl (*S*)-(1-(methoxy(methyl)amino)-1-oxopropan-2-yl)carbamate (18a).

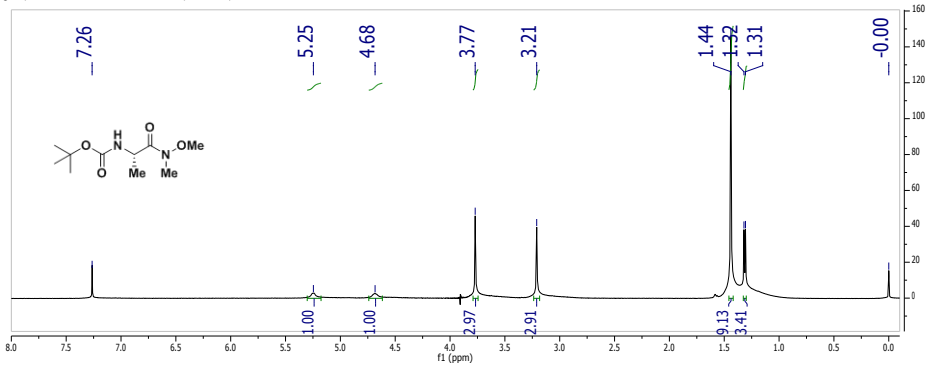

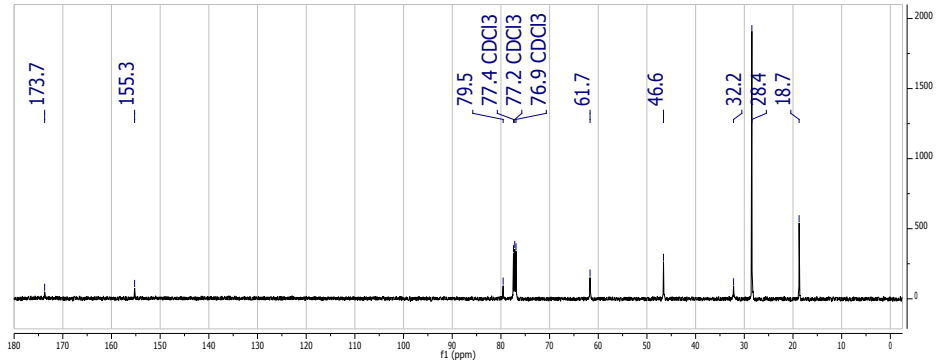

S7. ^{1}H and ^{13}C-NMR spectra of *tert*-butyl (*S*)-(1-(methoxy(methyl)amino)-1-oxo-3-phenylpropan-2-yl)carbamate (18b).

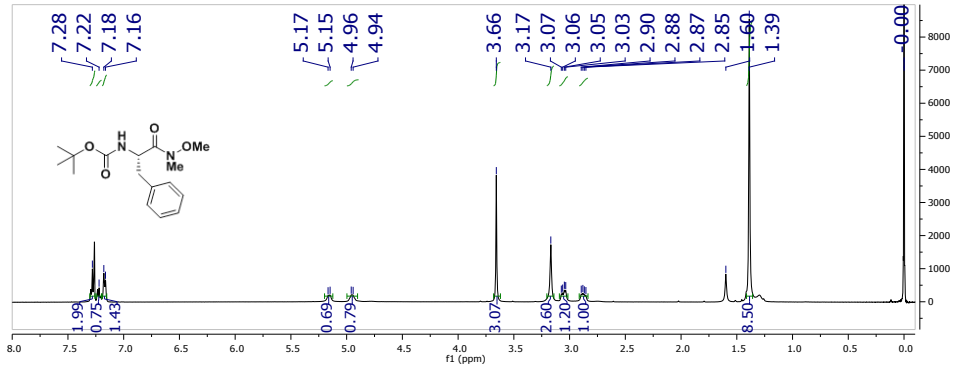

Trace water contamination at 1.6 ppm.

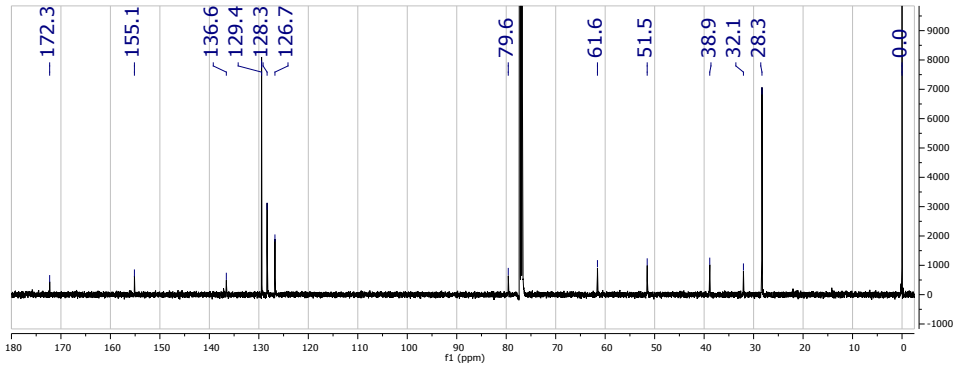

S8. ^{1}H and ^{13}C-NMR spectra of *tert*-butyl (*S*)-(1-(methoxy(methyl)amino)-1-oxo-3-phenylpropan-2-yl)carbamate (18c).

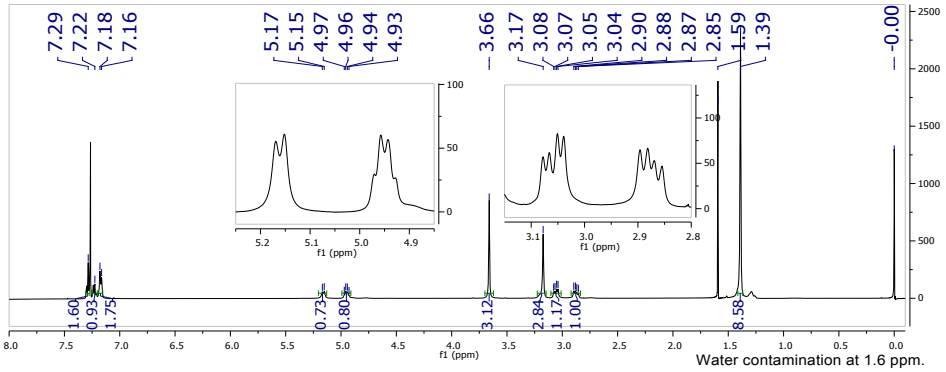

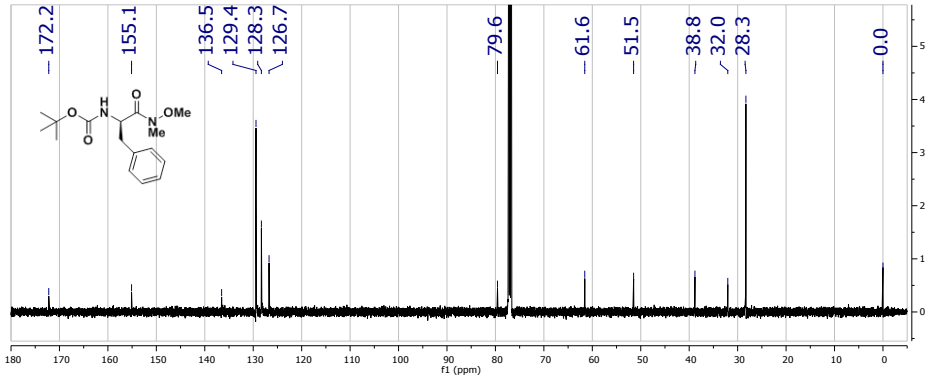

S9. ^{1}H and ^{13}C-NMR spectra of methyl (*S*,*E*)-4-((*tert*-butoxycarbonyl)amino)pent-2-enoate (19a).

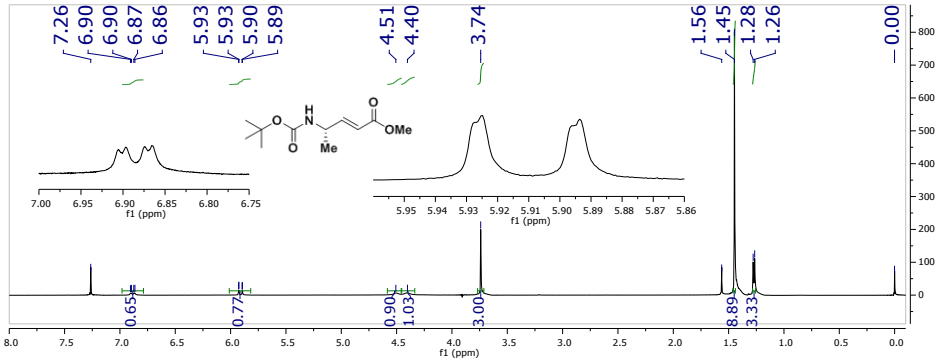

Trace water contamination at 1.6 ppm.

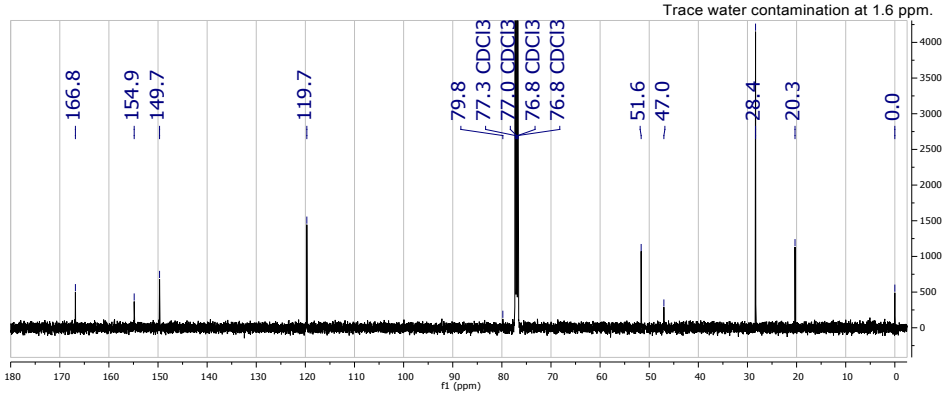

S10. ^{1}H and ^{13}C-NMR spectra of methyl (*S*,*E*)-4-((*tert*-butoxycarbonyl)amino)-5-phenylpent-2-enoate (19b).

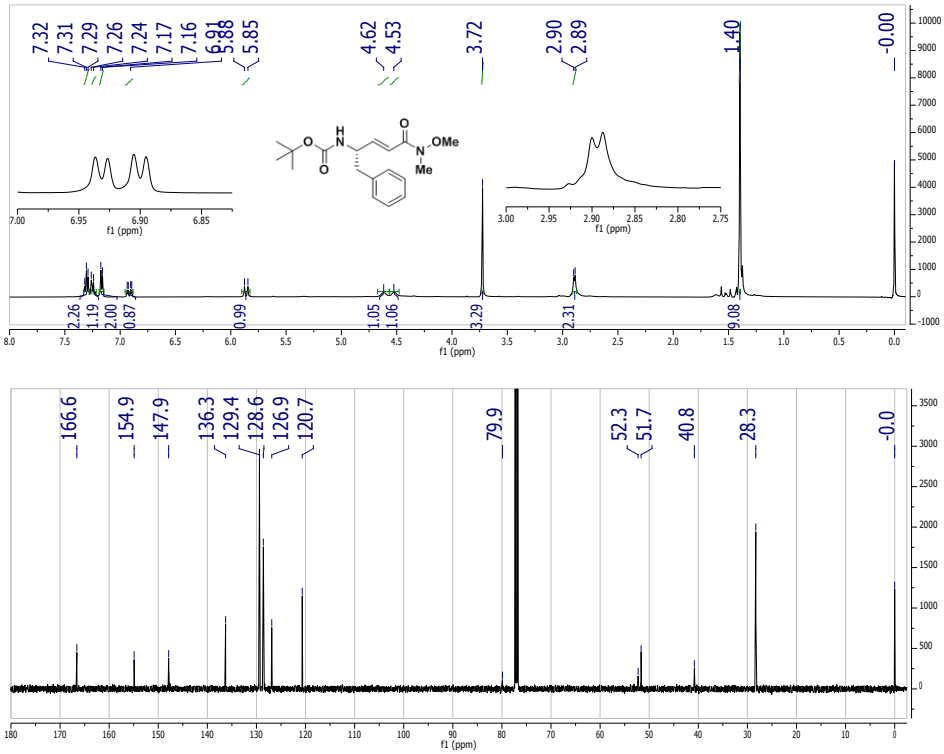

S11. ^{1}H and ^{13}C-NMR spectra of methyl (*R*,*E*)-4-((*tert*-butoxycarbonyl)amino)-5-phenylpent-2-enoate (19c).

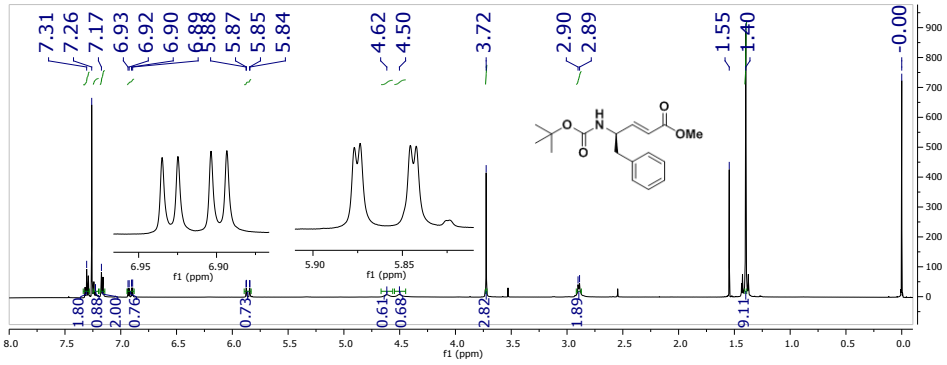

Water contamination at 1.6 ppm.

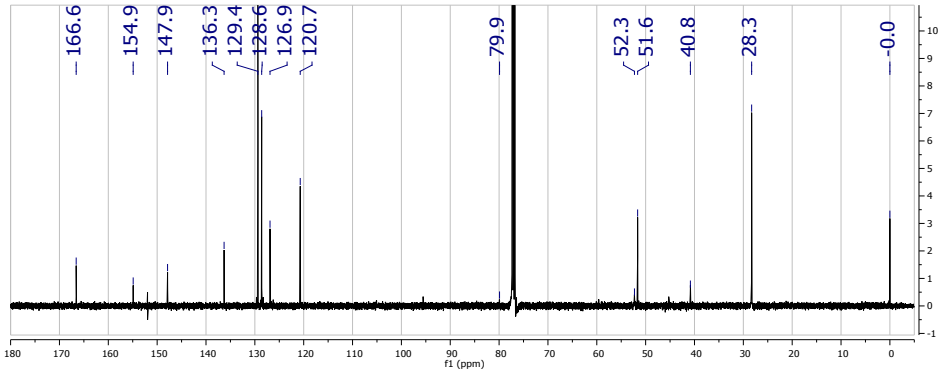

S12. ^{1}H and ^{13}C-NMR spectra of methyl ((*S*,*E*)-4-((*tert*-butoxycarbonyl)amino)pent-2-enoyl)-*L*-alaninate (23a).

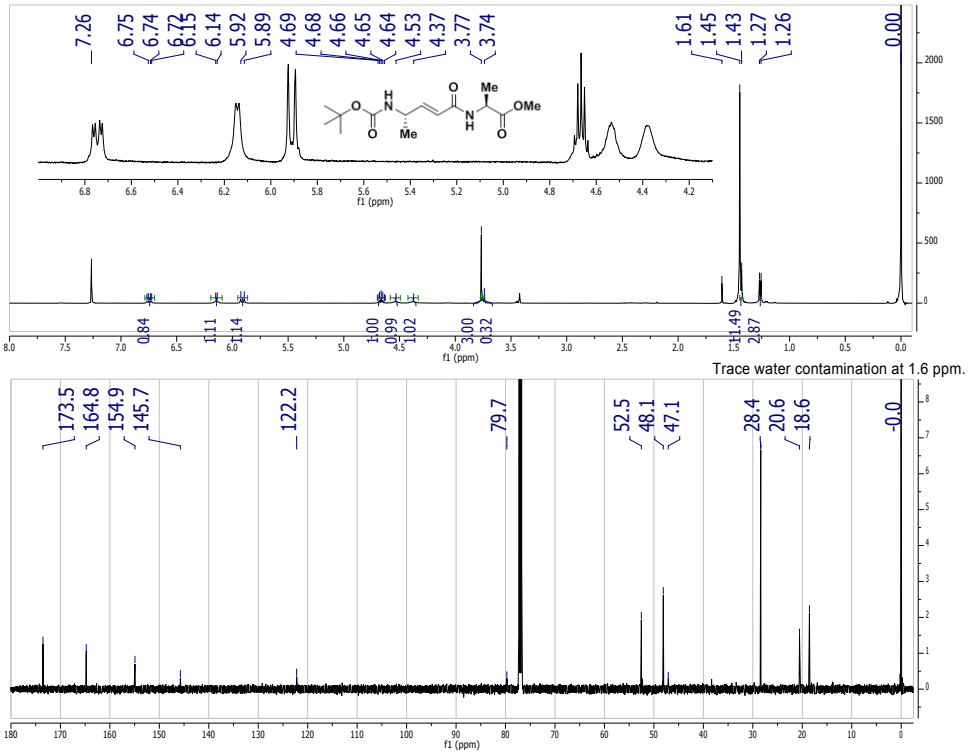

S13. ^{1}H and ^{13}C-NMR spectra of methyl ((*S*,*E*)-4-((*tert*-butoxycarbonyl)amino)pent-2-enoyl)-*L*-phenylalaninate (23b).

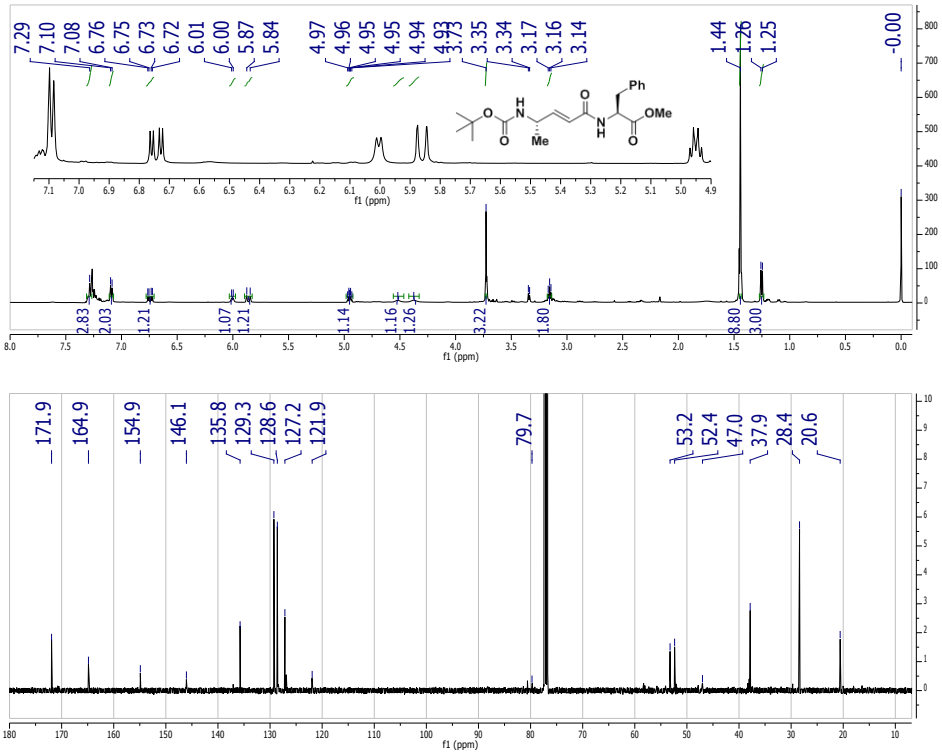

S14. ^{1}H and ^{13}C-NMR spectra of methyl ((*S*,*E*)-4-((*tert*-butoxycarbonyl)amino)pent-2-enoyl)-*L*-leucinate (23c).

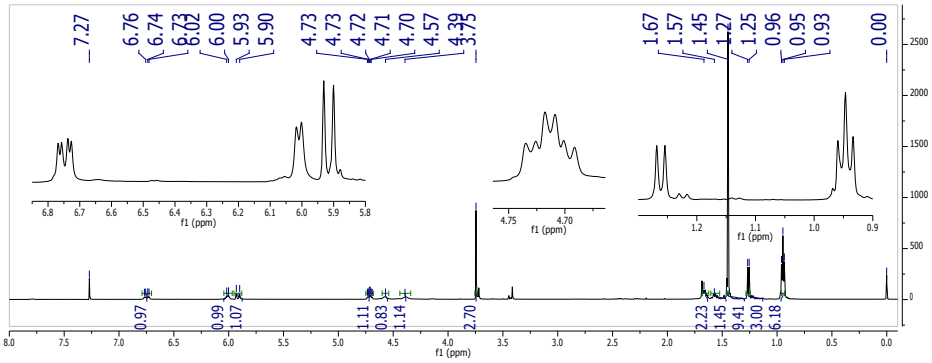

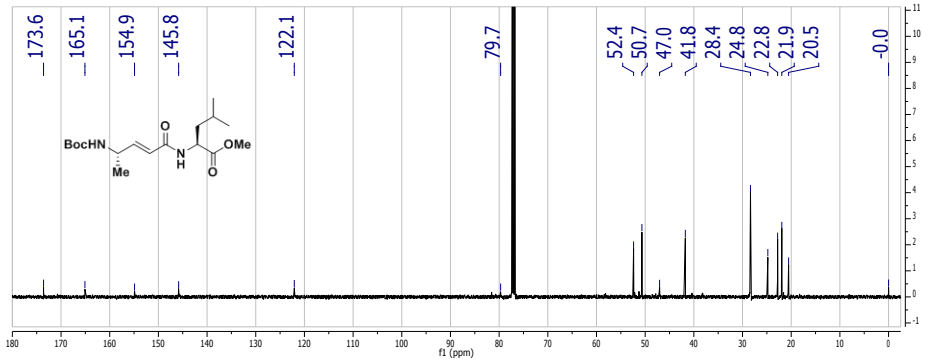

S15. ^{1}H and ^{13}C-NMR spectra of methyl ((*S*,*E*)-4-((*tert*-butoxycarbonyl)amino)-5-phenylpent-2-enoyl)-*L*-alaninate (23d).

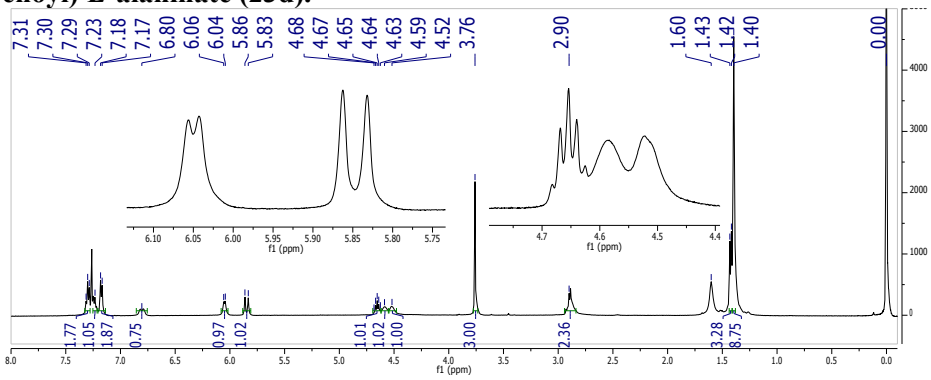

Water contamination at 1.6 ppm.

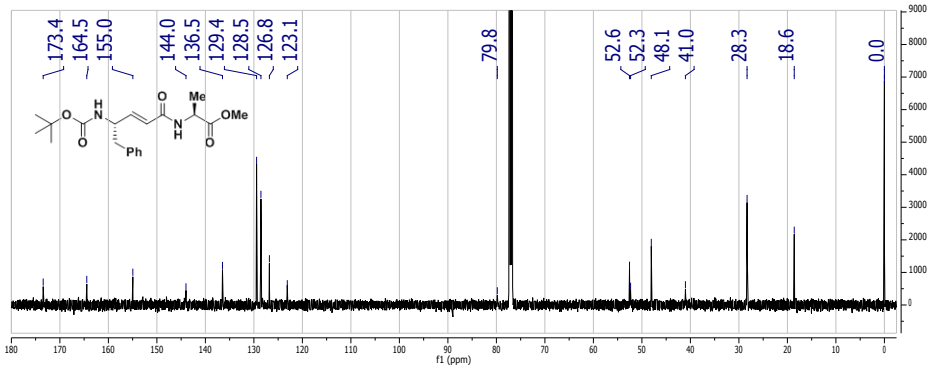

S16. ^{1}H and ^{13}C-NMR spectra of methyl ((*S*,*E*)-4-((*tert*-butoxycarbonyl)amino)-5-phenylpent-2-enoyl)-*L*-phenyl-alaninate (23e).

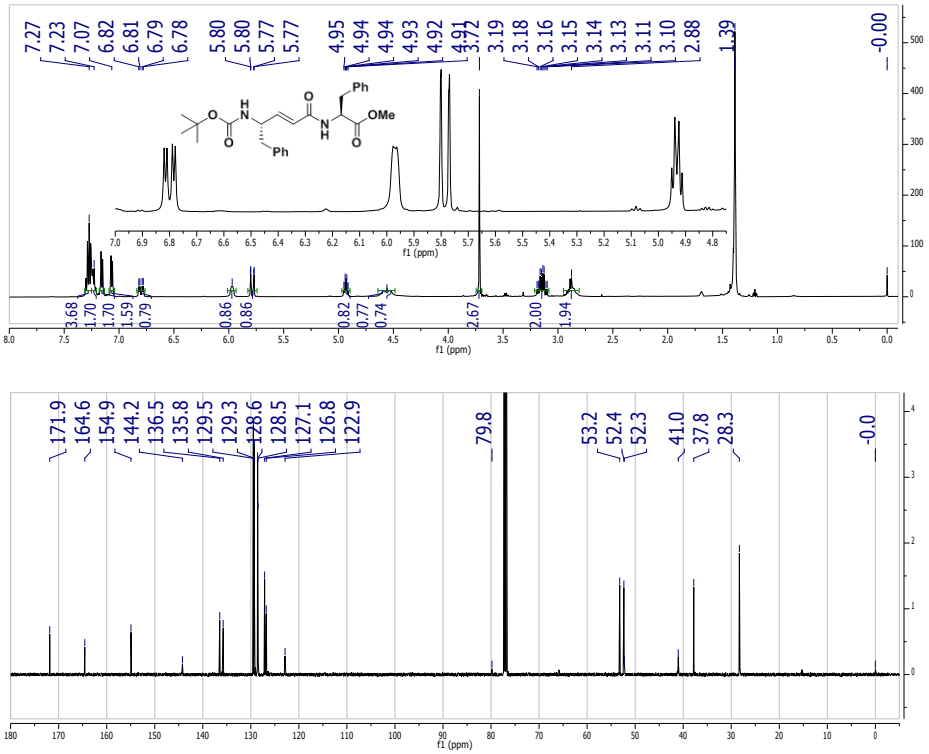

S17. ^{1}H and ^{13}C-NMR spectra of methyl ((*S*,*E*)-4-((*tert*-butoxycarbonyl)amino)-5-phenylpent-2-enoyl)-*L*-leucinate (23f).

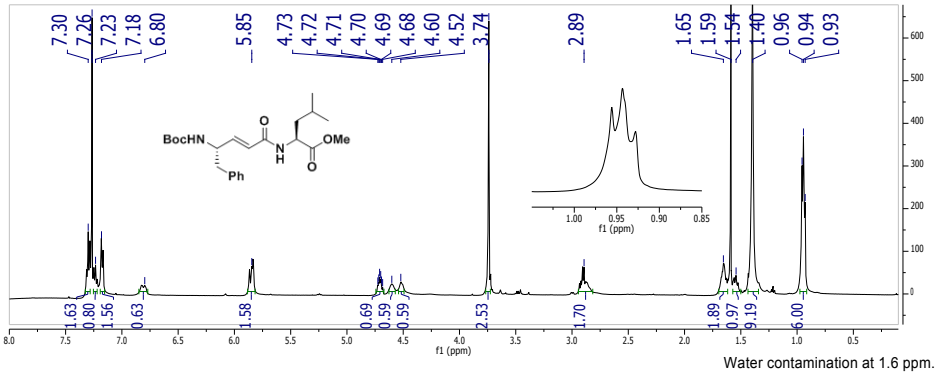

Water contamination at 1.6 ppm.

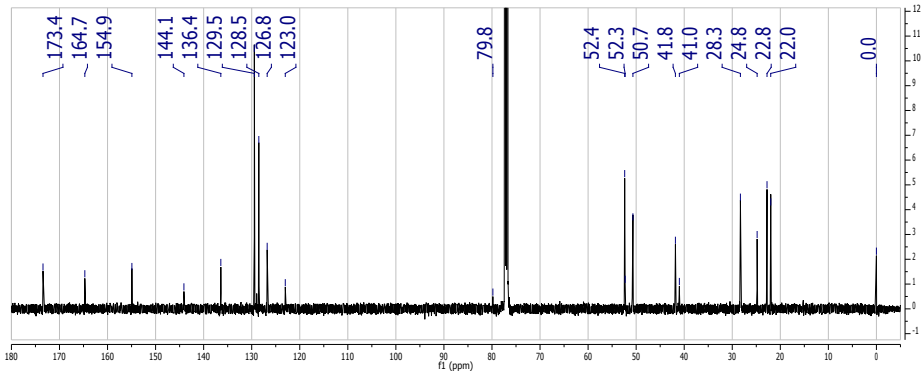

S18. ^{1}H and ^{13}C-NMR spectra of methyl ((*S*,*E*)-4-((*tert*-butoxycarbonyl)amino)-5-phenylpent-2-enoyl)-*D*-phenyl-alaninate (23g).

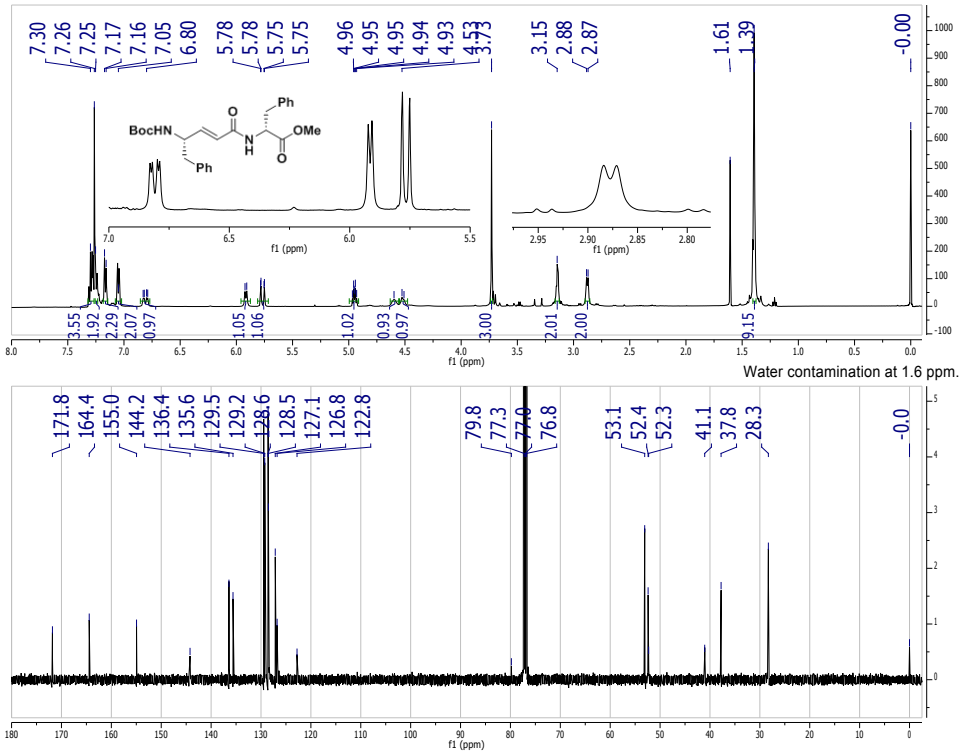

S19. ^{1}H and ^{13}C-NMR spectra of methyl ((*R*,*E*)-4-((*tert*-butoxycarbonyl)amino)-5-phenylpent-2-enoyl)-*L*-phenyl-alaninate (23h).

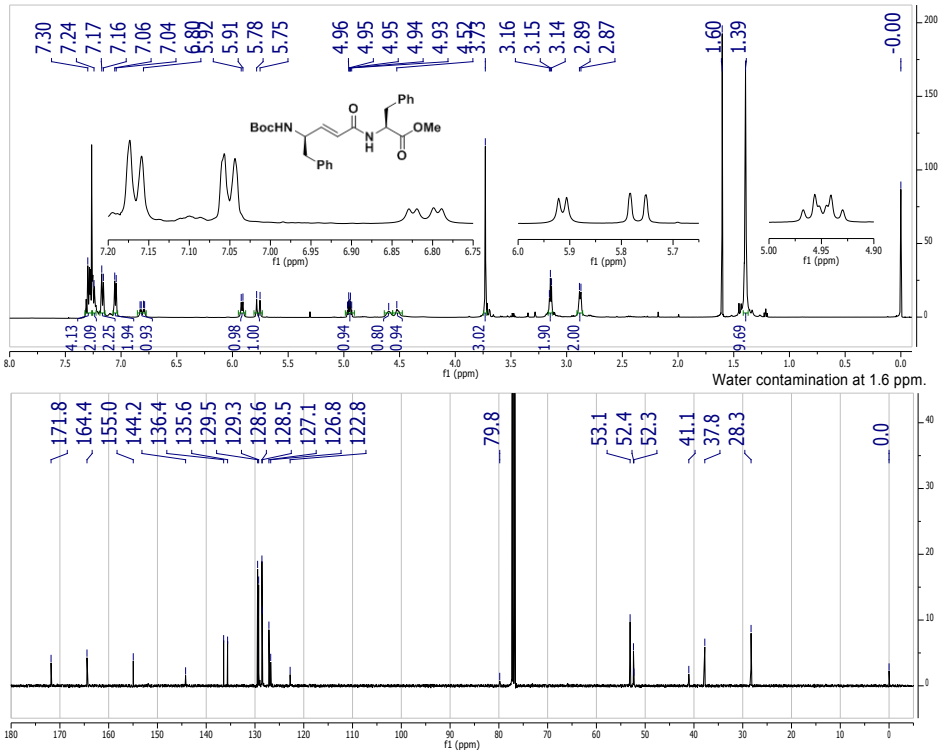

S20. ^{1}H and ^{13}C-NMR spectra methyl ((*R*,*E*)-4-((*tert*-butoxycarbonyl)amino)-5-phenylpent-2-enoyl)-*D*-phenyl-alaninate (23i).

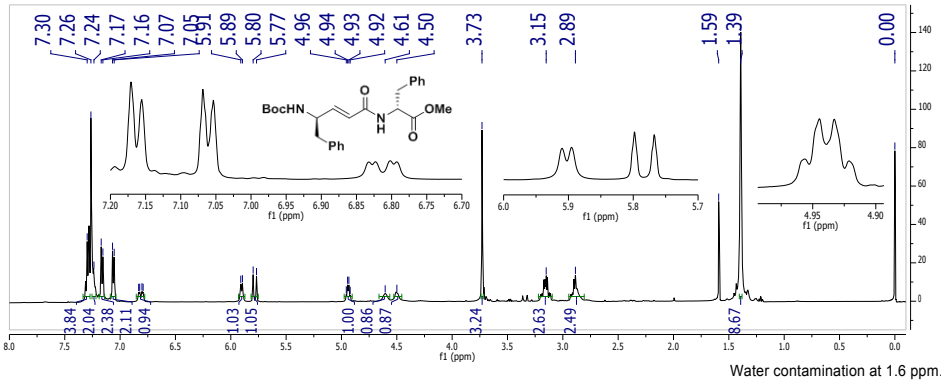

Water contamination at 1.6 ppm.

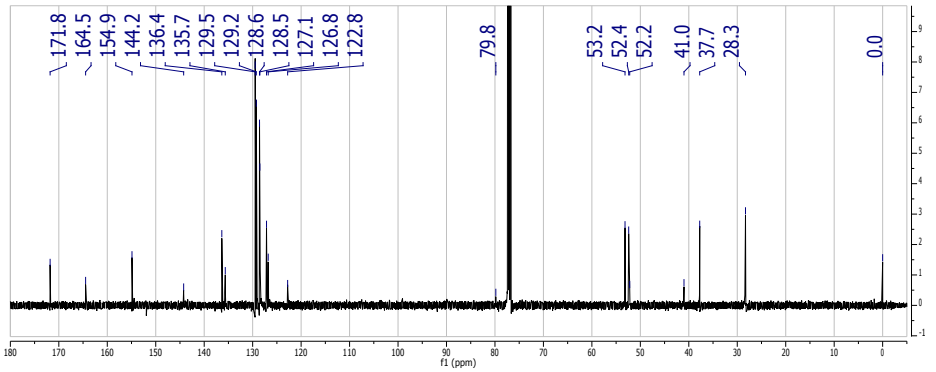

S21. ^{1}H and ^{13}C-NMR spectra *tert*-butyl ((*S*,*E*)-5-((*S*)-3-methoxy-2-methyl-5-oxo-2,5-dihydro-1*H*-pyrrol-1-yl)-5-oxopent-3-en-2-yl)carbamate (24a).

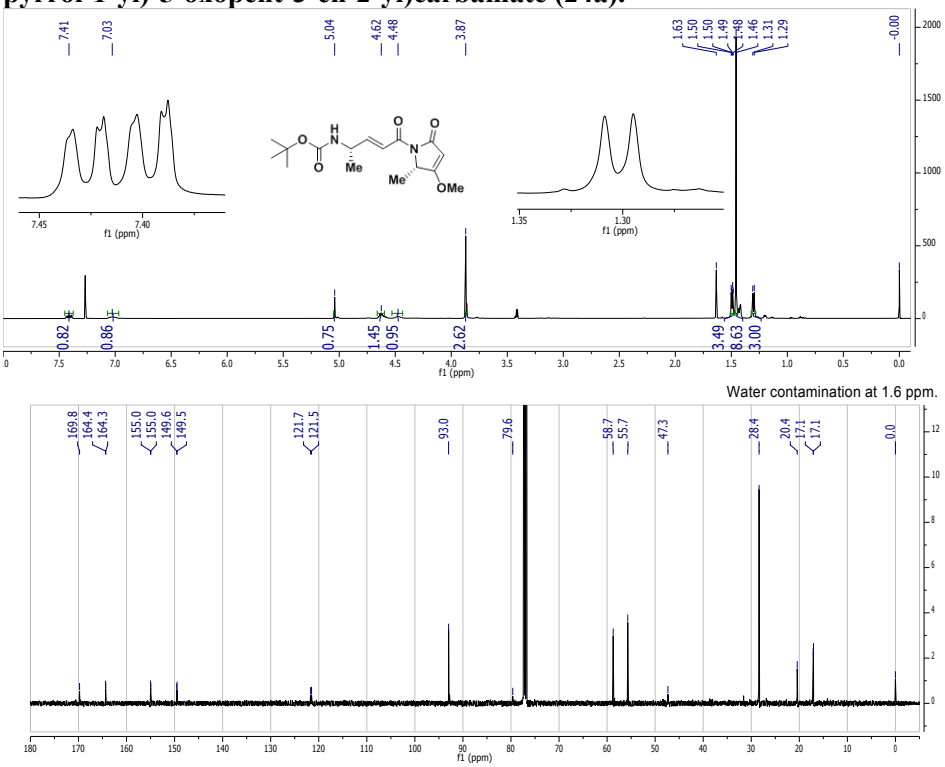

S22. ^{1}H and ^{13}C-NMR spectra of *tert*-butyl ((*S*,*E*)-5-((*S*)-2-benzyl-3-methoxy-5-oxo-2,5-dihydro-1*H*-pyrrol-1-yl)-5-oxopent-3-en-2-yl)carbamate (24b).

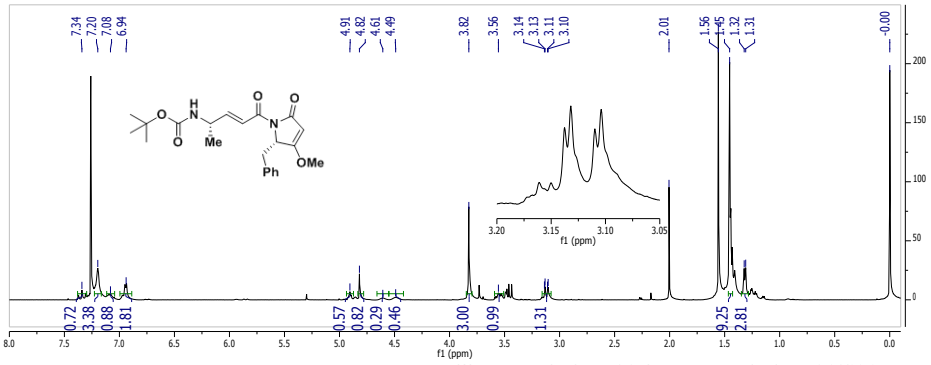

Water contamination at 1.6, Acetone contamination at 2.01/30.3 ppm.

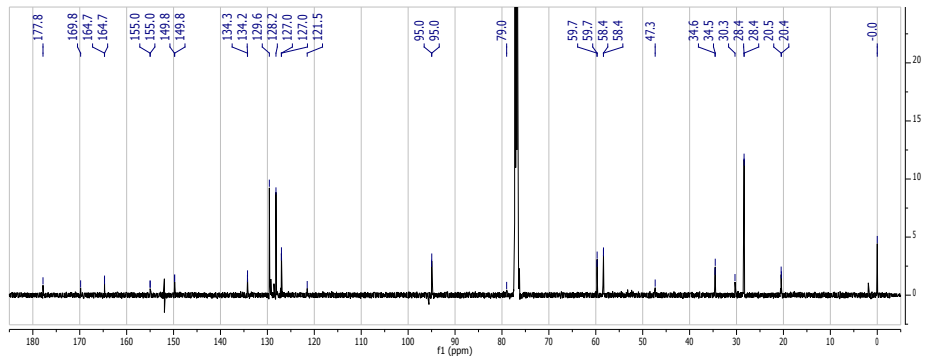

S23. ^{1}H and ^{13}C-NMR spectra of *tert*-butyl ((*S*,*E*)-5-((*S*)-2-isobutyl-3-methoxy-5-oxo-2,5-dihydro-1*H*-pyrrol-1-yl)-5-oxopent-3-en-2-yl)carbamate (24c).

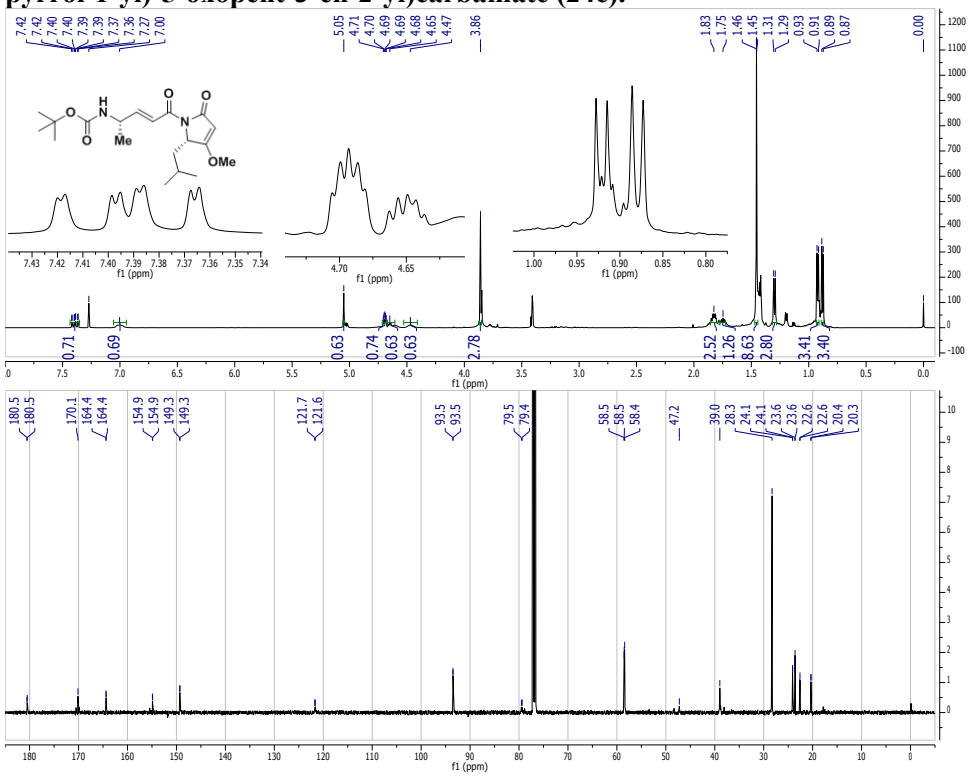

S24. ^{1}H and ^{13}C-NMR spectra of *tert*-butyl ((*S*,*E*)-5-((*S*)-3-methoxy-2-methyl-5-oxo-2,5-dihydro-1*H*-pyrrol-1-yl)-5-oxo-1-phenylpent-3-en-2-yl)carbamate (24d).

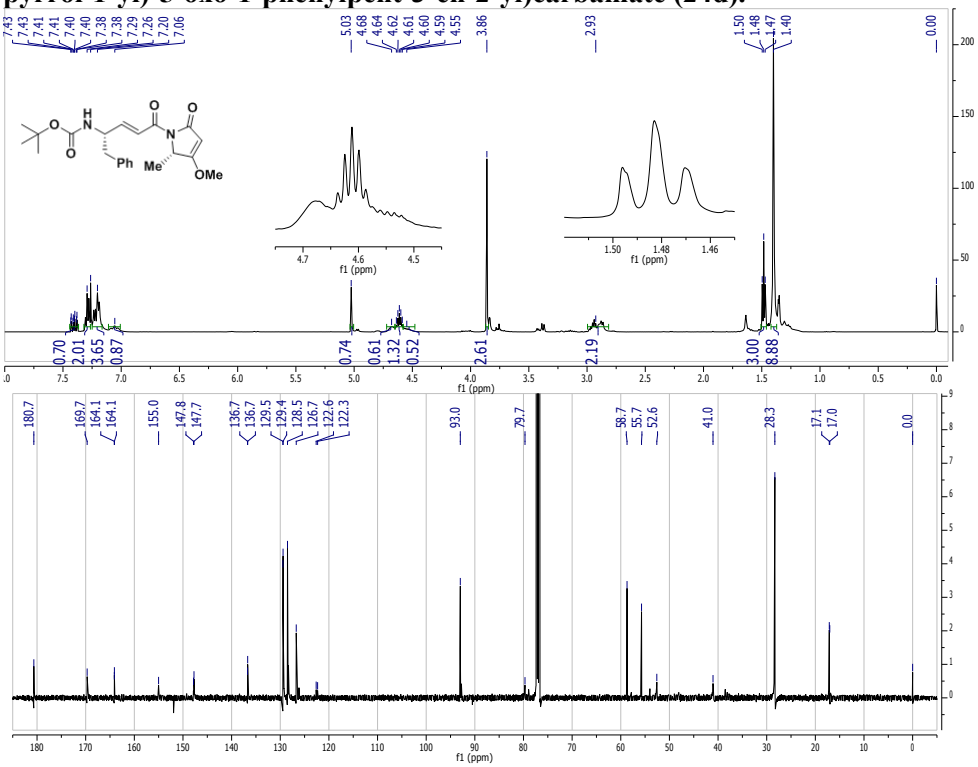

S25. ^{1}H and ^{13}C-NMR spectra of *tert*-butyl ((*S*,*E*)-5-((*S*)-2-benzyl-3-methoxy-5-oxo-2,5-dihydro-1*H*-pyrrol-1-yl)-5-oxo-1-phenylpent-3-en-2-yl)carbamate (24e).

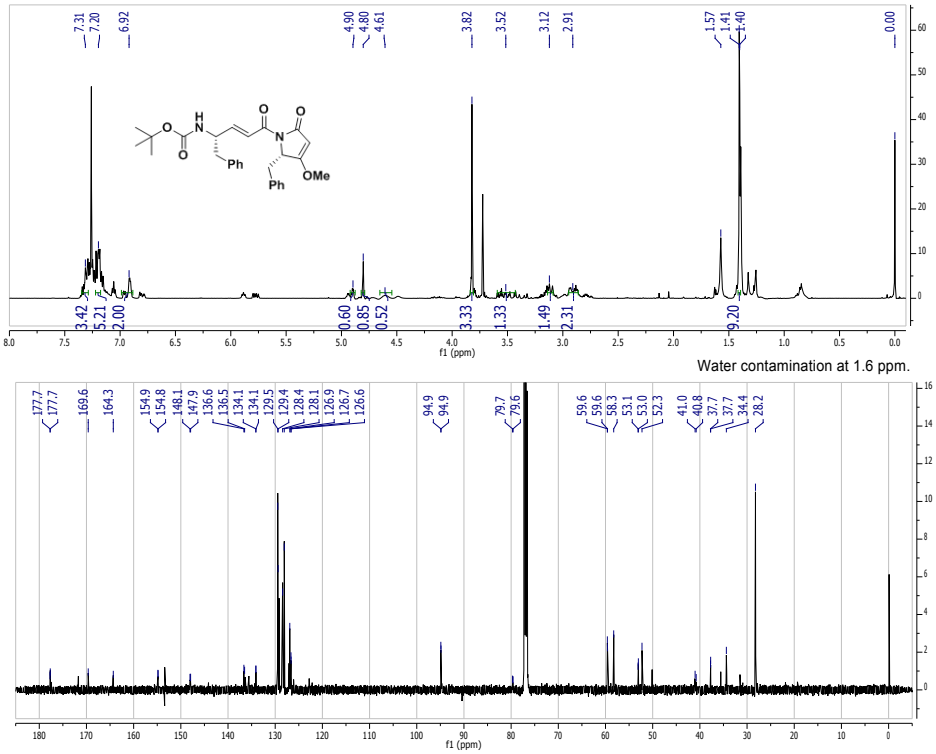

S26. ^{1}H and ^{13}C-NMR spectra of *tert*-butyl ((*S*,*E*)-5-((*S*)-2-isobutyl-3-methoxy-5-oxo-2,5-dihydro-1*H*-pyrrol-1-yl)-5-oxo-1-phenylpent-3-en-2-yl)carbamate (24f).

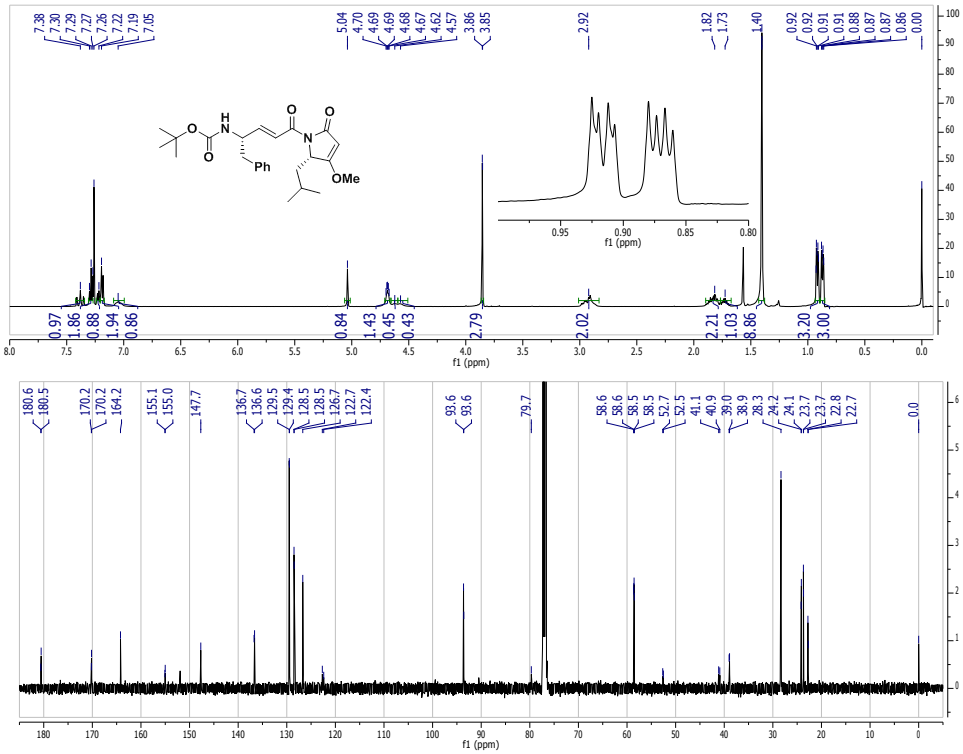

S27. ^{1}H and ^{13}C-NMR spectra of *tert*-butyl ((*S*,*E*)-5-((*R*)-2-benzyl-3-methoxy-5-oxo-2,5-dihydro-1*H*-pyrrol-1-yl)-5-oxo-1-phenylpent-3-en-2-yl)carbamate (24g).

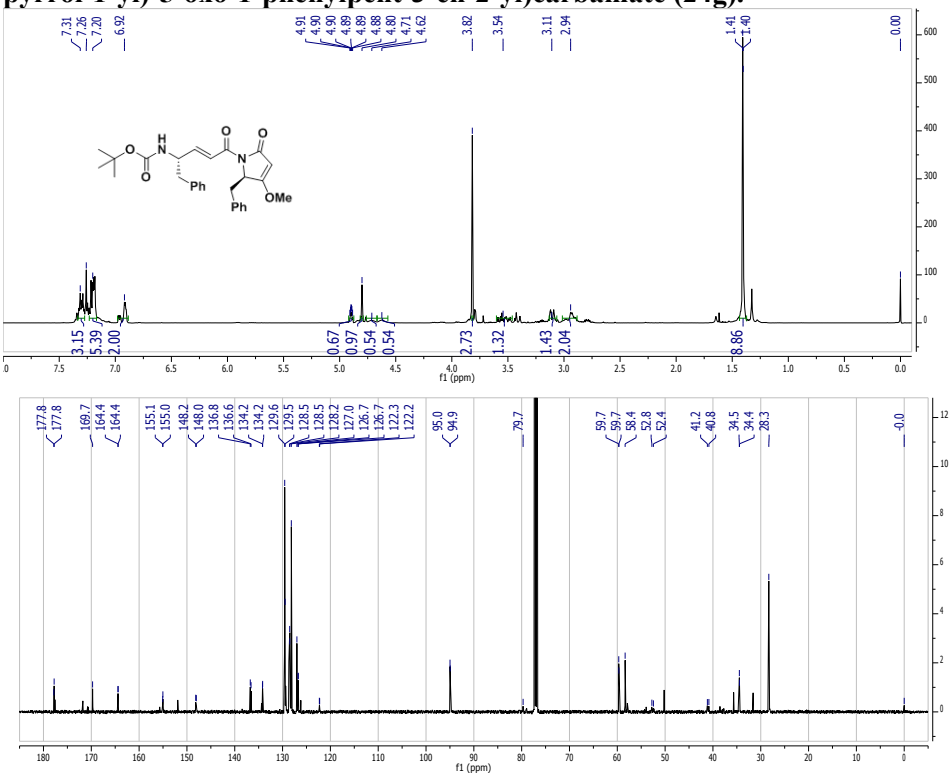

S28. ^{1}H and ^{13}C-NMR spectra of *tert*-butyl ((*R*,*E*)-5-((*S*)-2-benzyl-3-methoxy-5-oxo-2,5-dihydro-1*H*-pyrrol-1-yl)-5-oxo-1-phenylpent-3-en-2-yl)carbamate (24h).

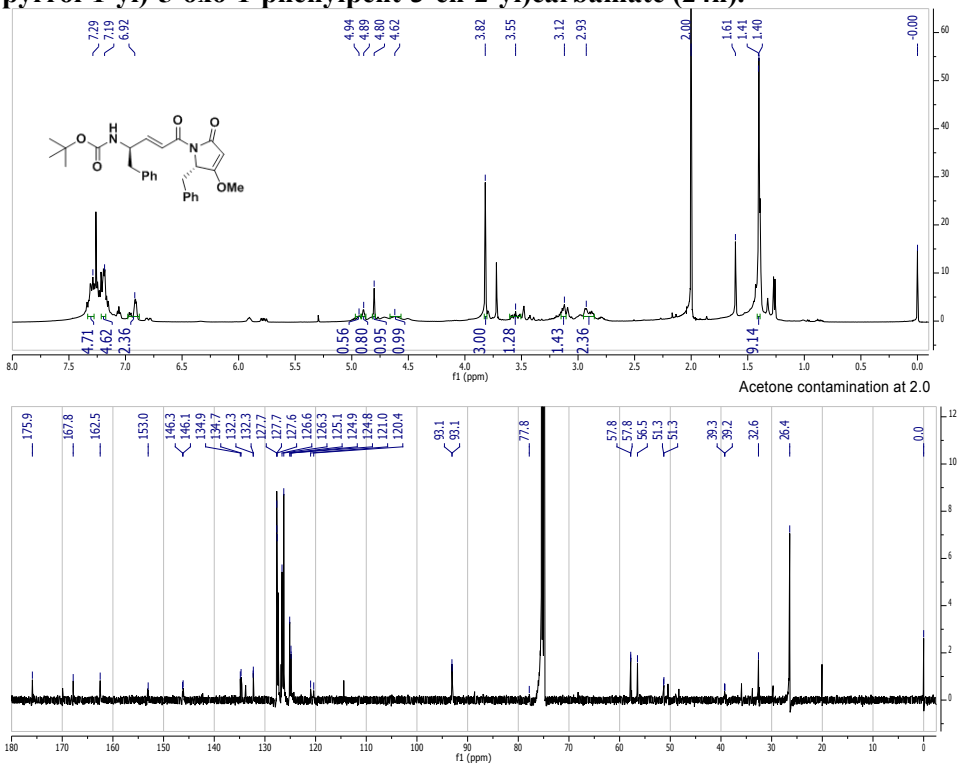

S29. ^{1}H and ^{13}C-NMR spectra of *tert*-butyl ((*R*,*E*)-5-((*R*)-2-benzyl-3-methoxy-5-oxo-2,5-dihydro-1*H*-pyrrol-1-yl)-5-oxo-1-phenylpent-3-en-2-yl)carbamate (24i).

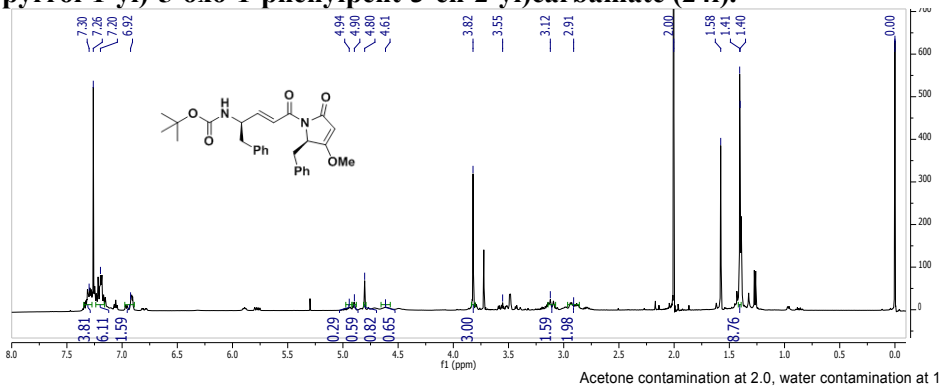

Acetone contamination at 2.0, water contamination at 1.6

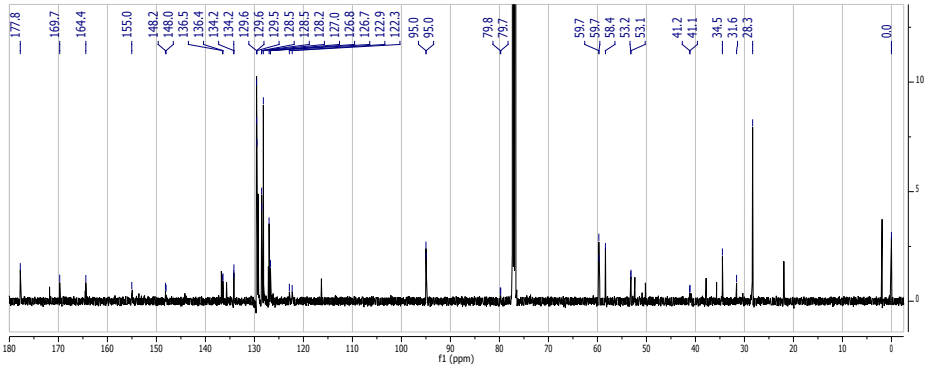

S30. ^{1}H and ^{13}C-NMR spectra of *tert*-butyl ((*S*,*E*)-5-((*S*)-3-(hex-5-yn-1-yloxy)-2-methyl-5-oxo-2,5-dihydro-1*H*-pyrrol-1-yl)-5-oxopent-3-en-2-yl)carbamate (24j).

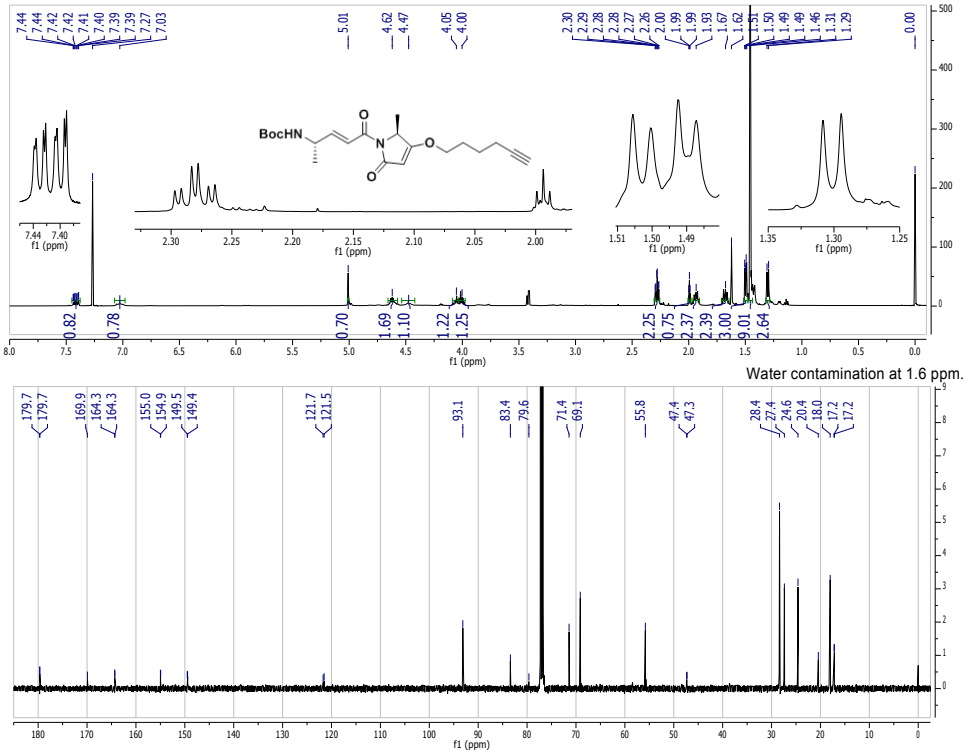

S31. ^{1}H and ^{13}C-NMR spectra of *tert*-butyl ((*S*)-1-(((*S*,*E*)-5-((*S*)-3-methoxy-2-methyl-5-oxo-2,5-dihydro-1*H*-pyrrol-1-yl)-5-oxopent-3-en-2-yl)amino)-4-methyl-1-oxopentan-2-yl)carbamate (25a).

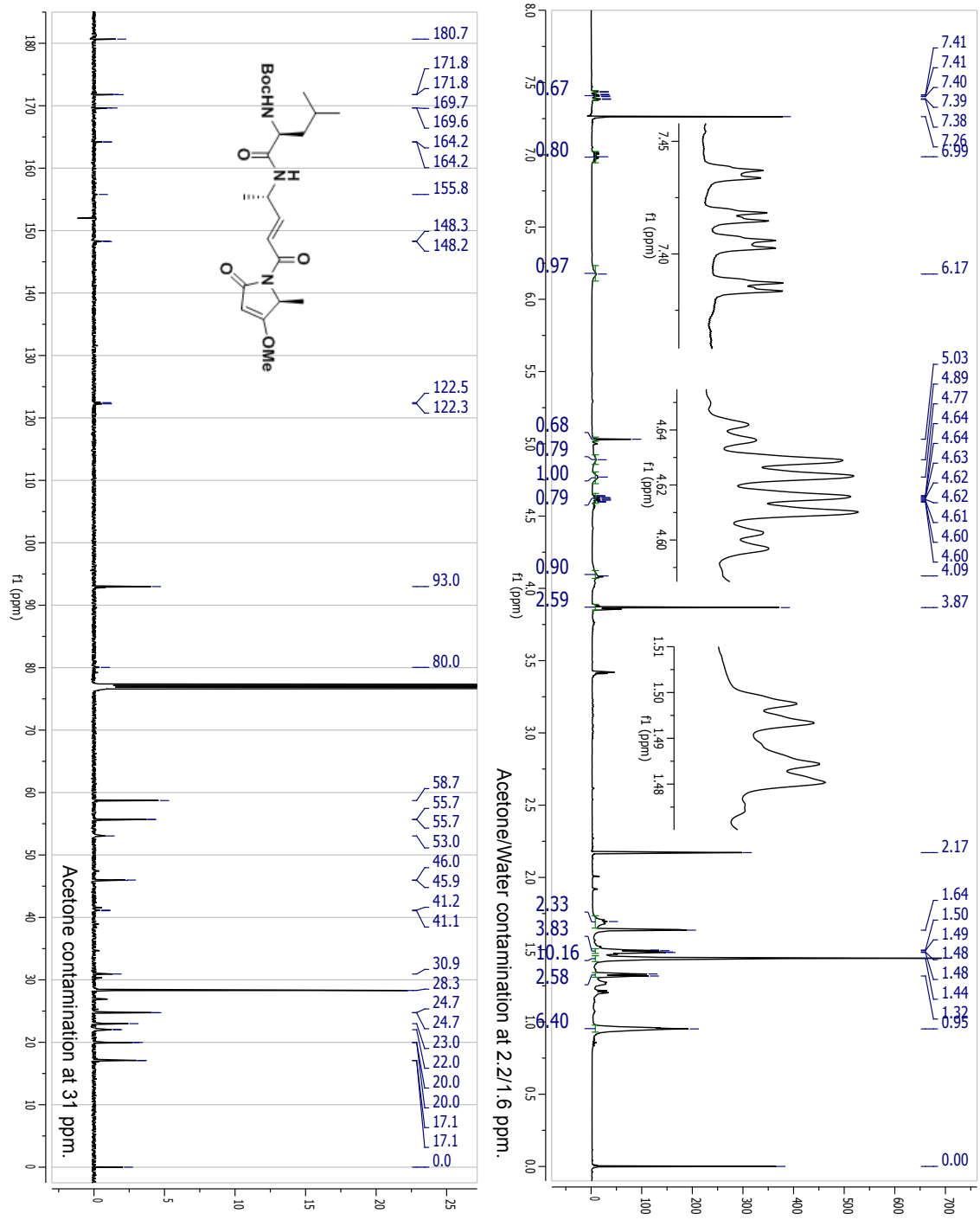

S32. ^{1}H and ^{13}C-NMR spectra of *tert*-butyl ((*S*)-1-(((*S*,*E*)-5-((*S*)-2-benzyl-3-methoxy-5-oxo-2,5-dihydro-1*H*-pyrrol-1-yl)-5-oxopent-3-en-2-yl)amino)-4-methyl-1-oxopentan-2-yl)carbamate (25b).

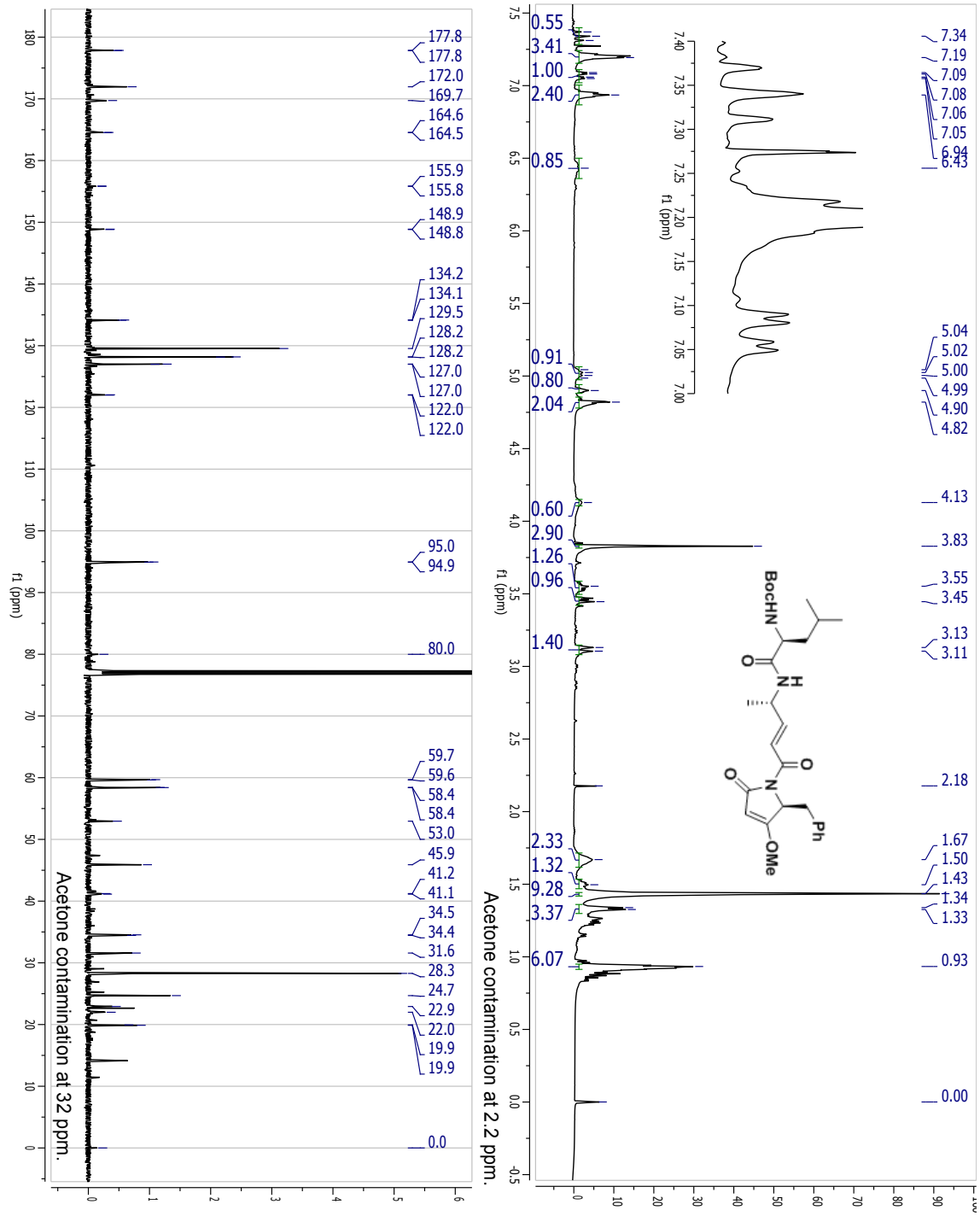

S33. ^{1}H and ^{13}C-NMR spectra of *tert*-butyl ((*S*)-1-(((*S*,*E*)-5-((*S*)-2-isobutyl-3-methoxy-5-oxo-2,5-dihydro-1*H*-pyrrol-1-yl)-5-oxopent-3-en-2-yl)amino)-4-methyl-1-oxopentan-2-yl)carbamate (25c).

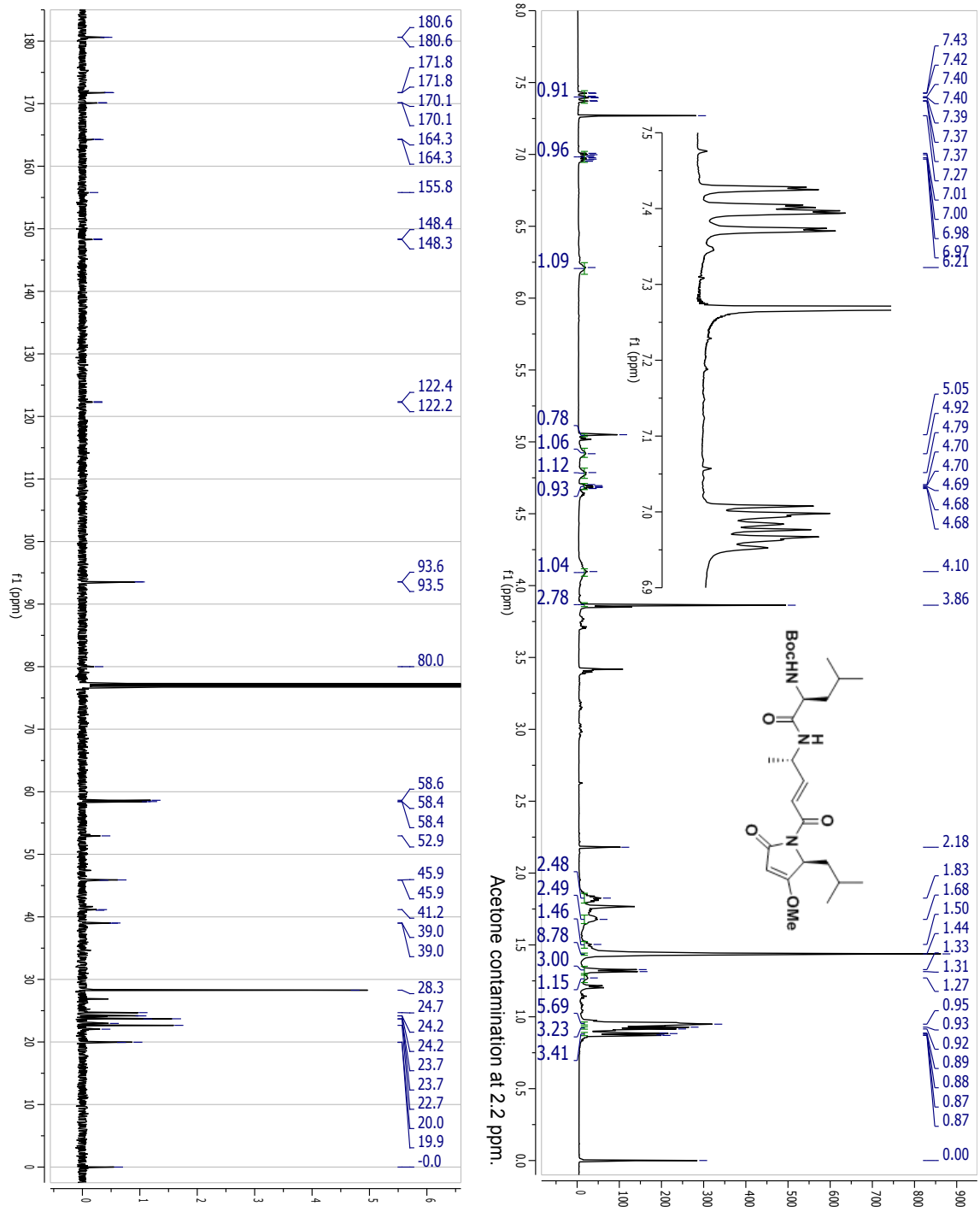

S34. ^{1}H and ^{13}C-NMR spectra of *tert*-butyl ((*S*)-1-(((*S*,*E*)-5-((*S*)-3-methoxy-2-methyl-5-oxo-2,5-dihydro-1*H*-pyrrol-1-yl)-5-oxo-1-phenylpent-3-en-2-yl)amino)-4-methyl-1-oxopentan-2-yl)carbamate (25d).

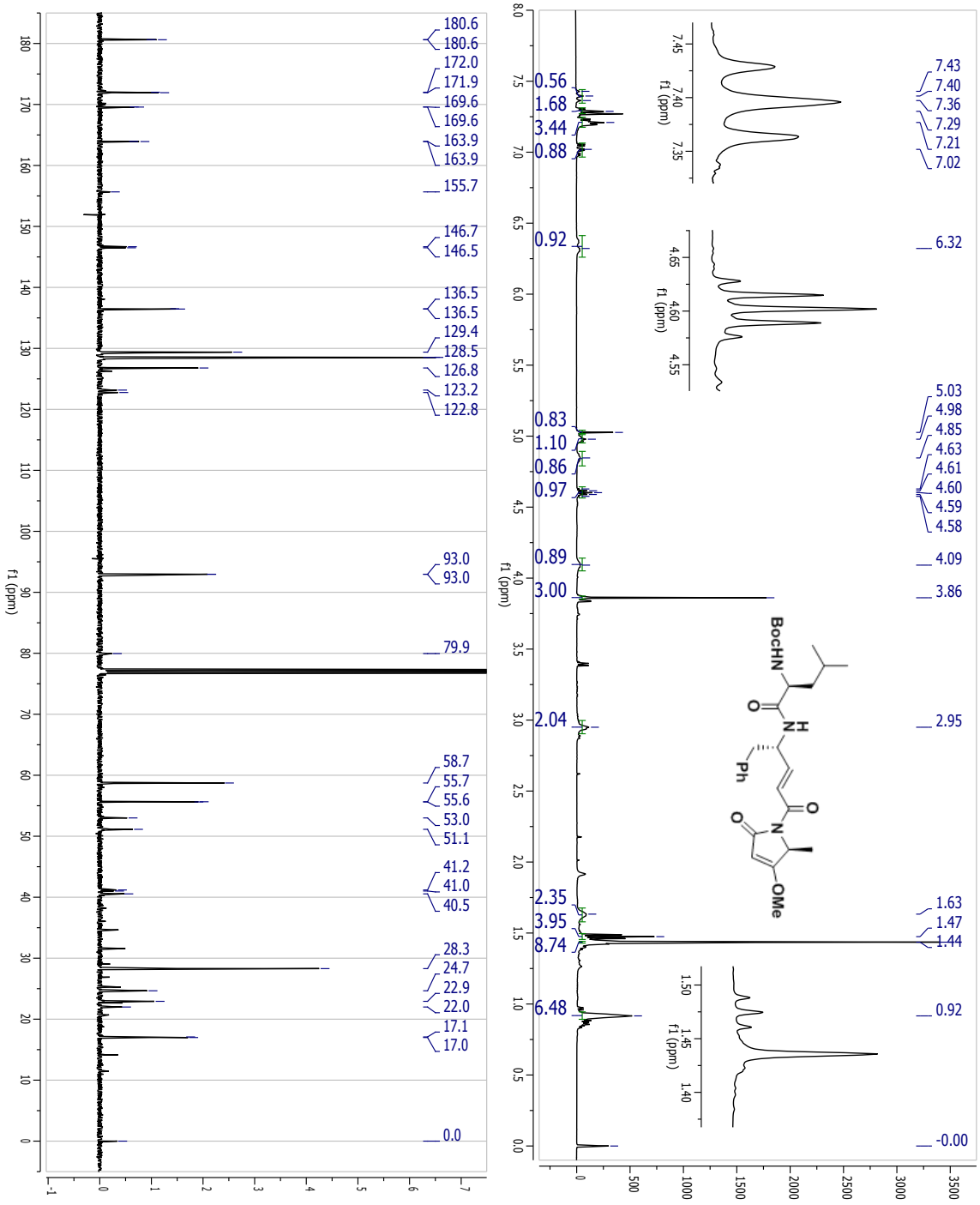

S35. ^{1}H and ^{13}C-NMR spectra *tert*-butyl ((*S*)-1-(((*S*,*E*)-5-((*S*)-2-benzyl-3-methoxy-5-oxo-2,5-dihydro-1*H*-pyrrol-1-yl)-5-oxo-1-phenylpent-3-en-2-yl)amino)-4-methyl-1-oxopentan-2-yl)carbamate (25e).

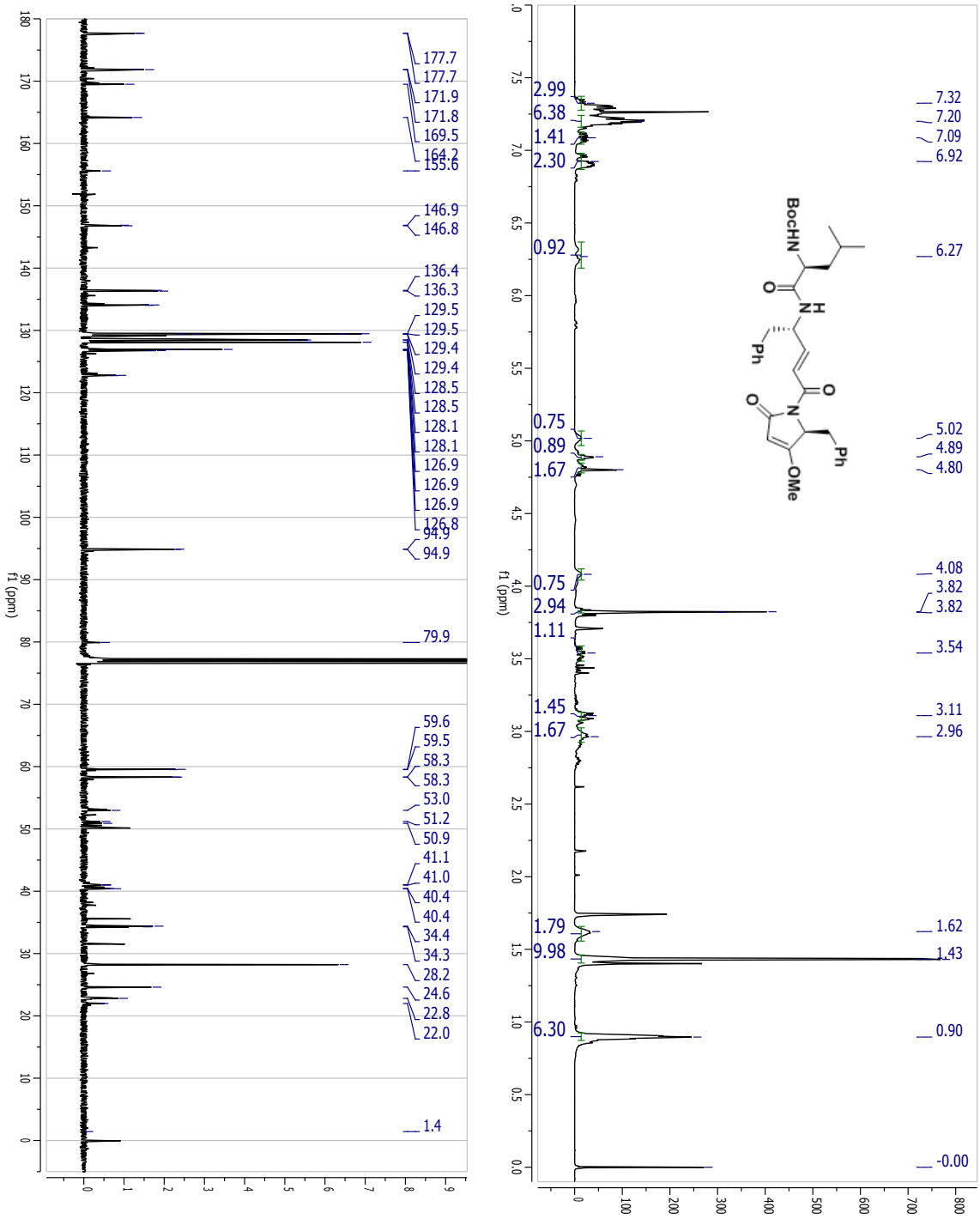

S36. ^{1}H and ^{13}C-NMR spectra *tert*-butyl ((*S*)-1-(((*S*,*E*)-5-((*S*)-2-isobutyl-3-methoxy-5-oxo-2,5-dihydro-1*H*-pyrrol-1-yl)-5-oxo-1-phenylpent-3-en-2-yl)amino)-4-methyl-1-oxopentan-2-yl)carbamate (25f).

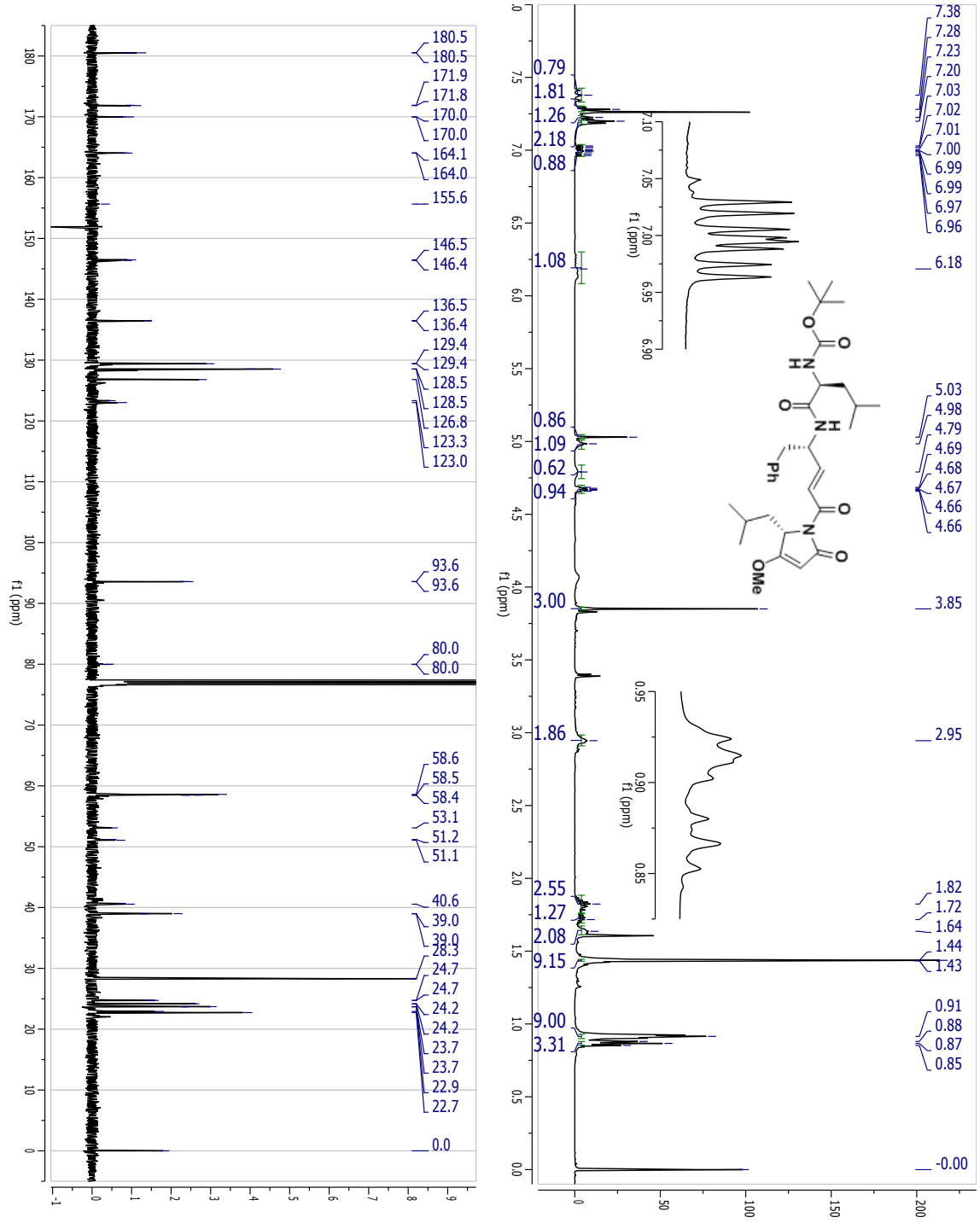

S37. ^{1}H and ^{13}C-NMR spectra *tert*-butyl ((*S*)-1-(((*S*,*E*)-5-((*R*)-2-benzyl-3-methoxy-5-oxo-2,5-dihydro-1*H*-pyrrol-1-yl)-5-oxo-1-phenylpent-3-en-2-yl)amino)-4-methyl-1-oxopentan-2-yl)carbamate (25g).

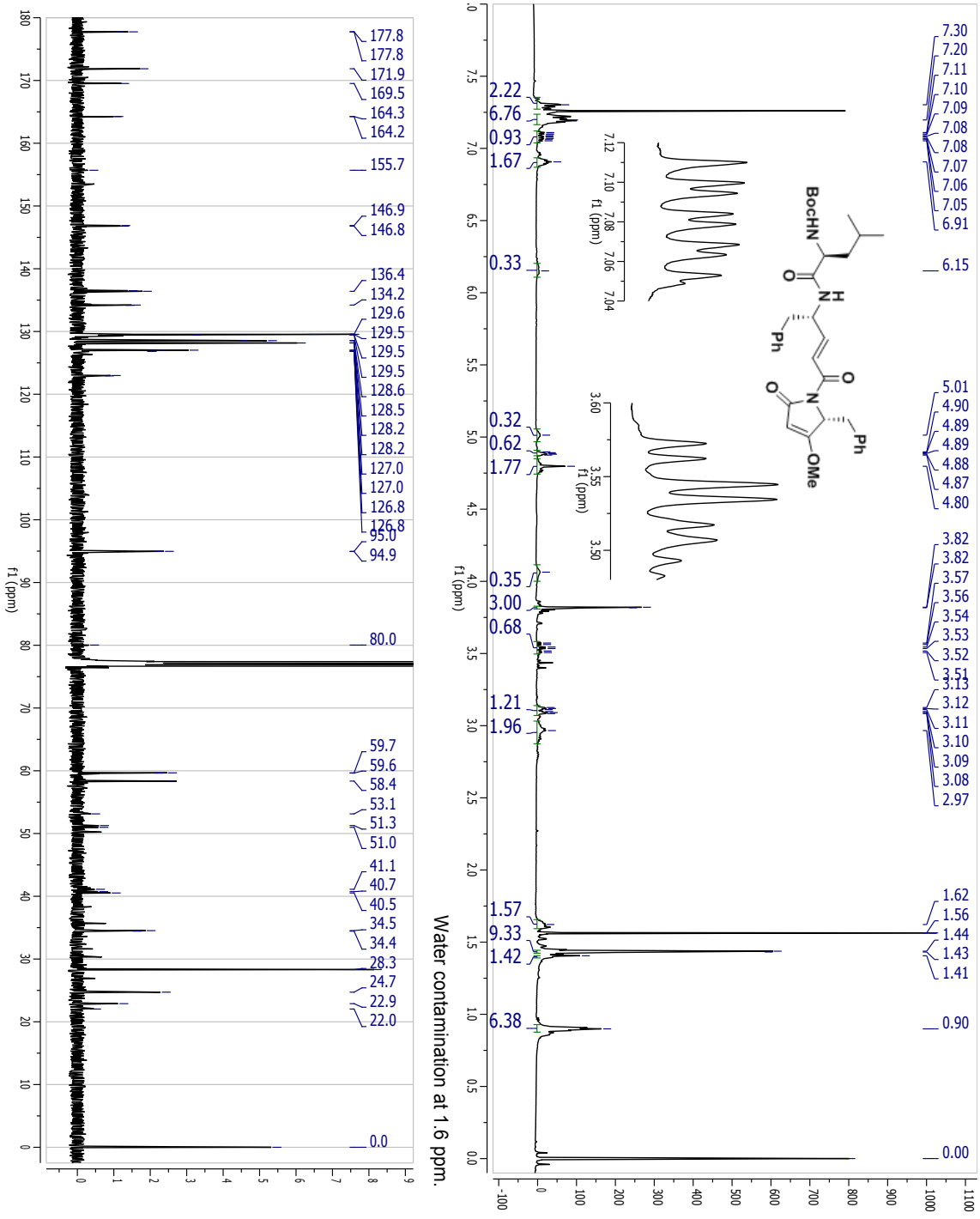

S38. ^{1}H and ^{13}C-NMR spectra *tert*-butyl ((*S*)-1-(((*R*,*E*)-5-((*S*)-2-benzyl-3-methoxy-5-oxo-2,5-dihydro-1*H*-pyrrol-1-yl)-5-oxo-1-phenylpent-3-en-2-yl)amino)-4-methyl-1-oxopentan-2-yl)carbamate (25h).

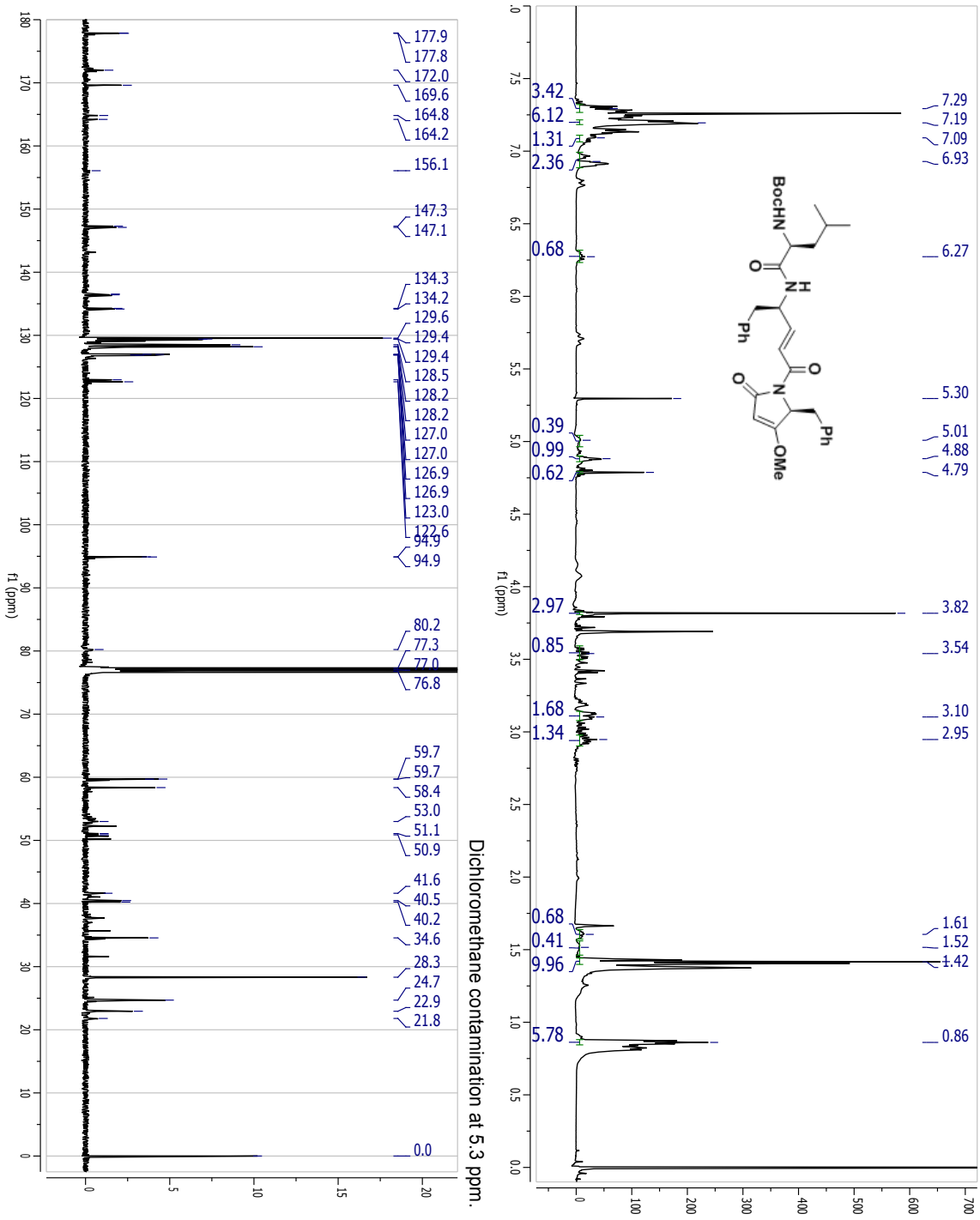

S39. ^{1}H and ^{13}C-NMR spectra *tert*-butyl ((*S*)-1-(((*R*,*E*)-5-((*R*)-2-benzyl-3-methoxy-5-oxo-2,5-dihydro-1*H*-pyrrol-1-yl)-5-oxo-1-phenylpent-3-en-2-yl)amino)-4-methyl-1-oxopentan-2-yl)carbamate (25i).

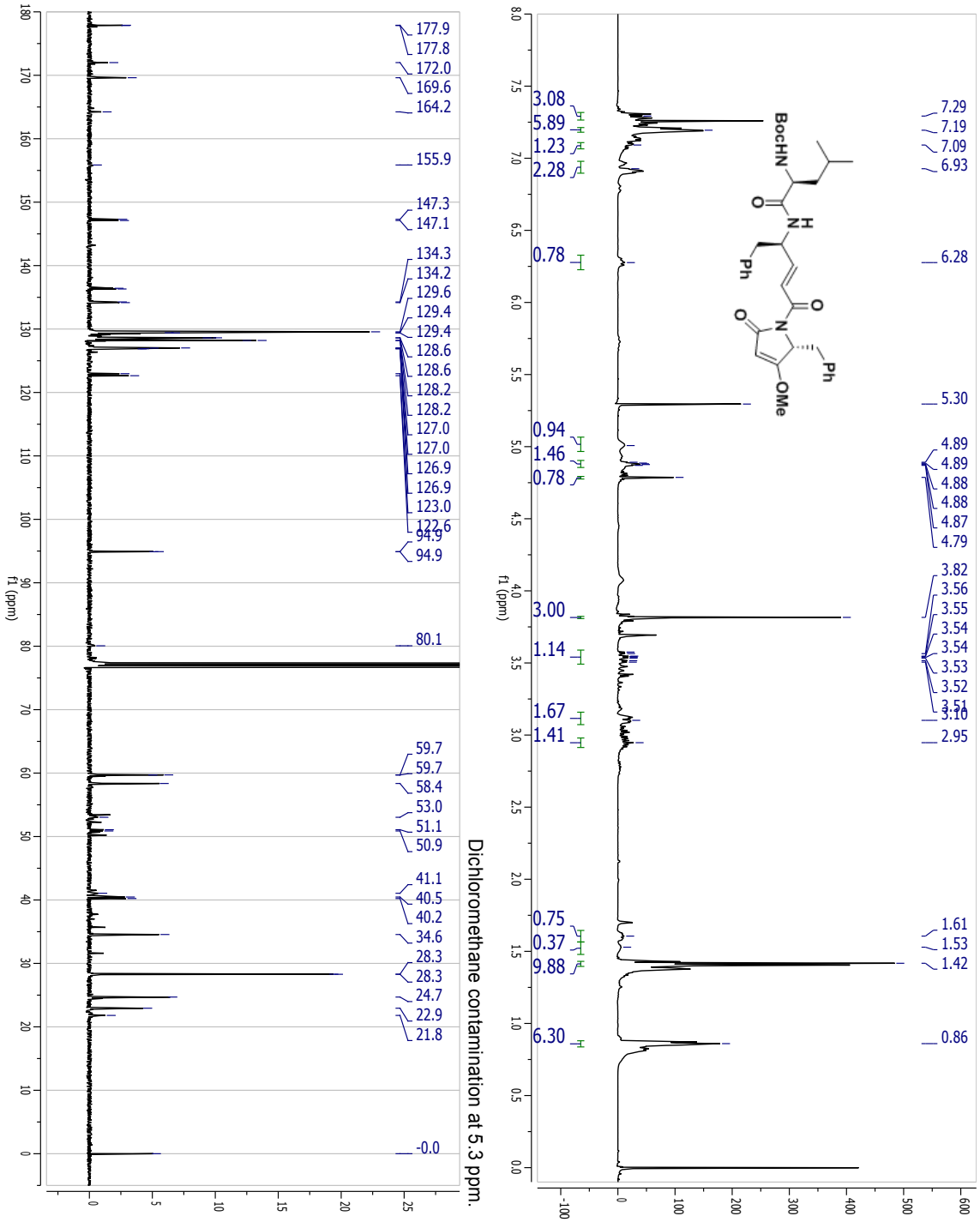

S40. ^{1}H and ^{13}C-NMR spectra of *tert*-butyl ((*S*)-1-(((*S*,*E*)-5-((*S*)-3-(hex-5-yn-1-yloxy)-2-methyl-5-oxo-2,5-dihydro-1*H*-pyrrol-1-yl)-5-oxopent-3-en-2-yl)amino)-4-methyl-1-oxopentan-2-yl)carbamate (25j).

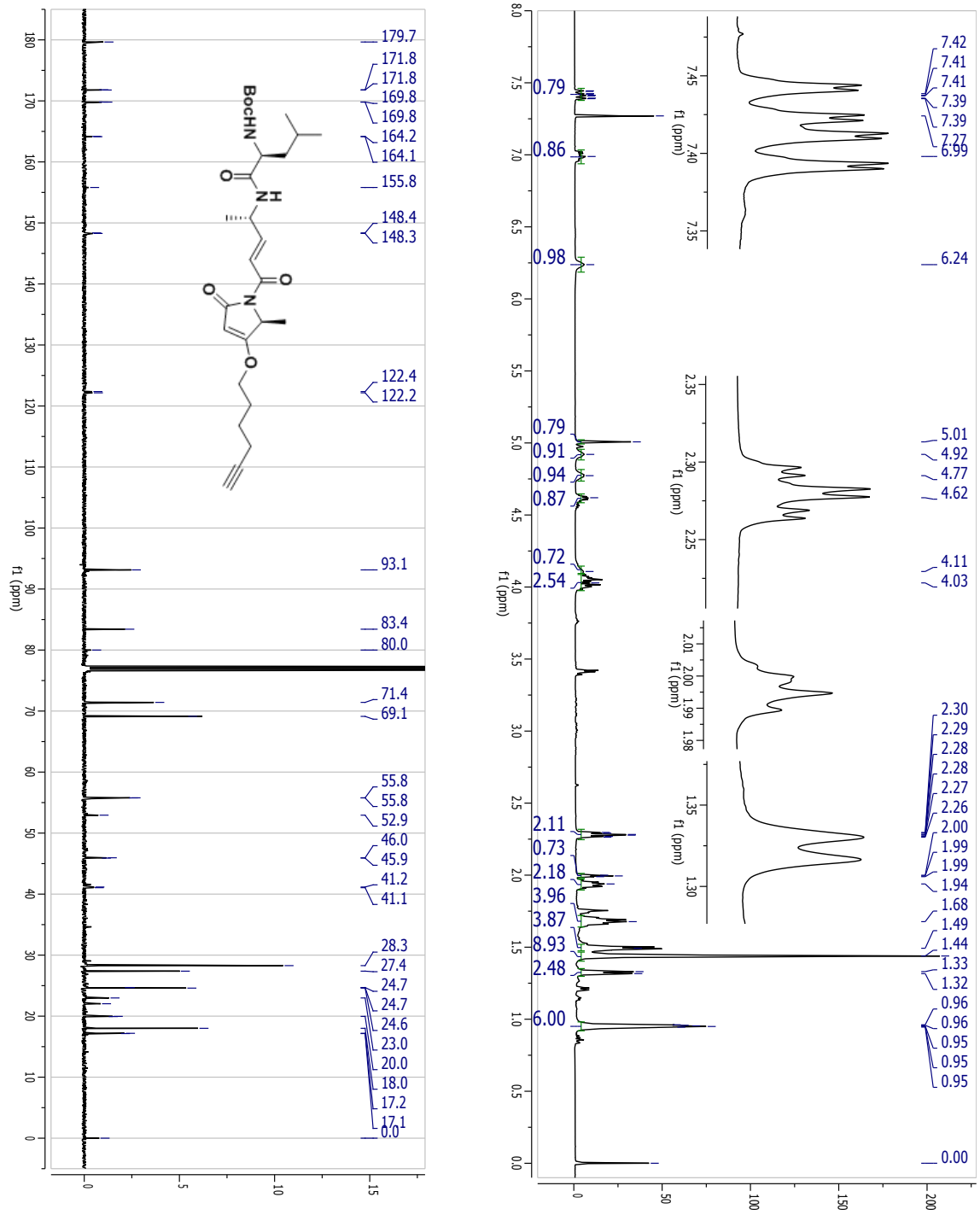

S41. ^{1}H and ^{13}C-NMR spectra of benzyl (*S*)-2-hydroxy-4-methylpentanoate (20).

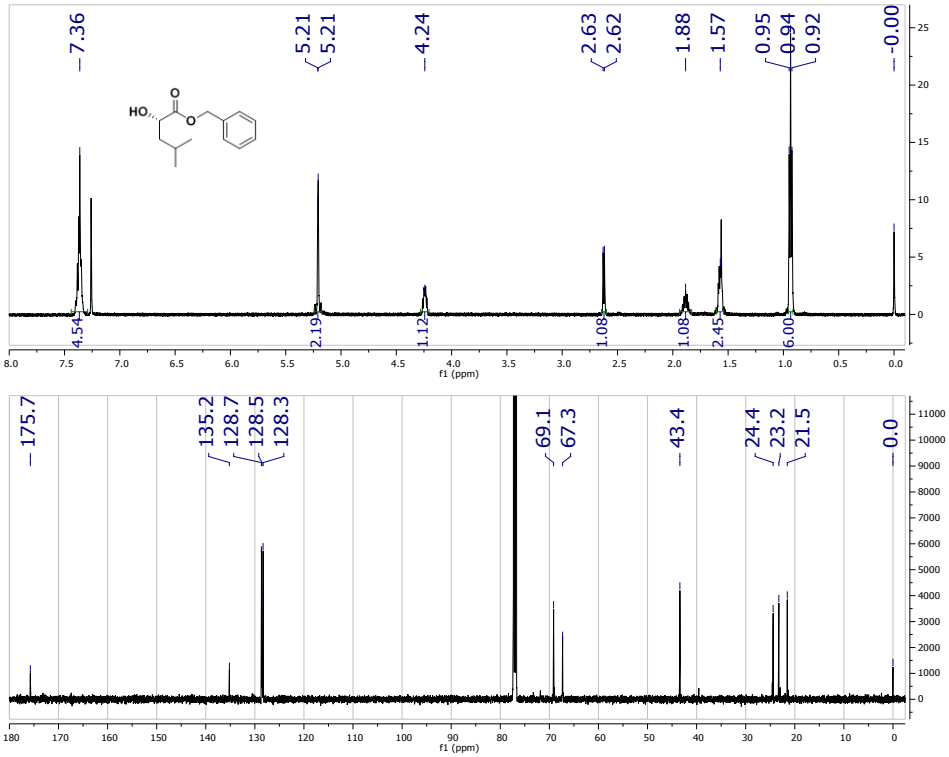

S42. ^{1}H and ^{13}C-NMR spectra of benzyl (*S*)-2-((*L*-isoleucyl)oxy)-4-methylpentanoate (21a).

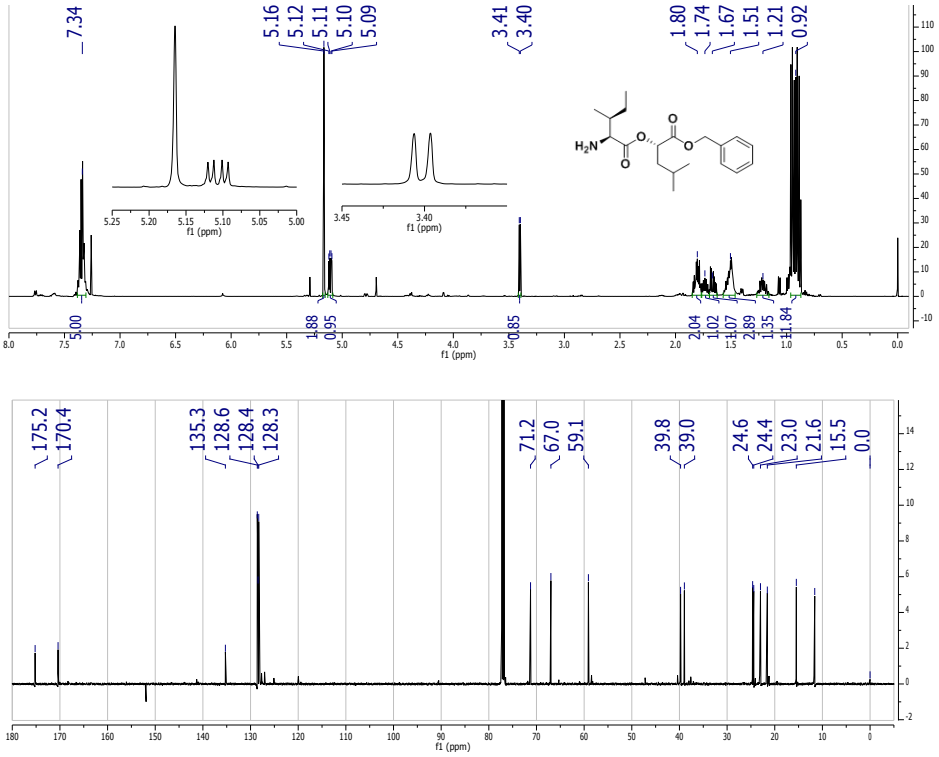

S43. ^{1}H and ^{13}C-NMR spectra of benzyl (*S*)-2-((*L*-valyl)oxy)-4-methylpentanoate (21b).

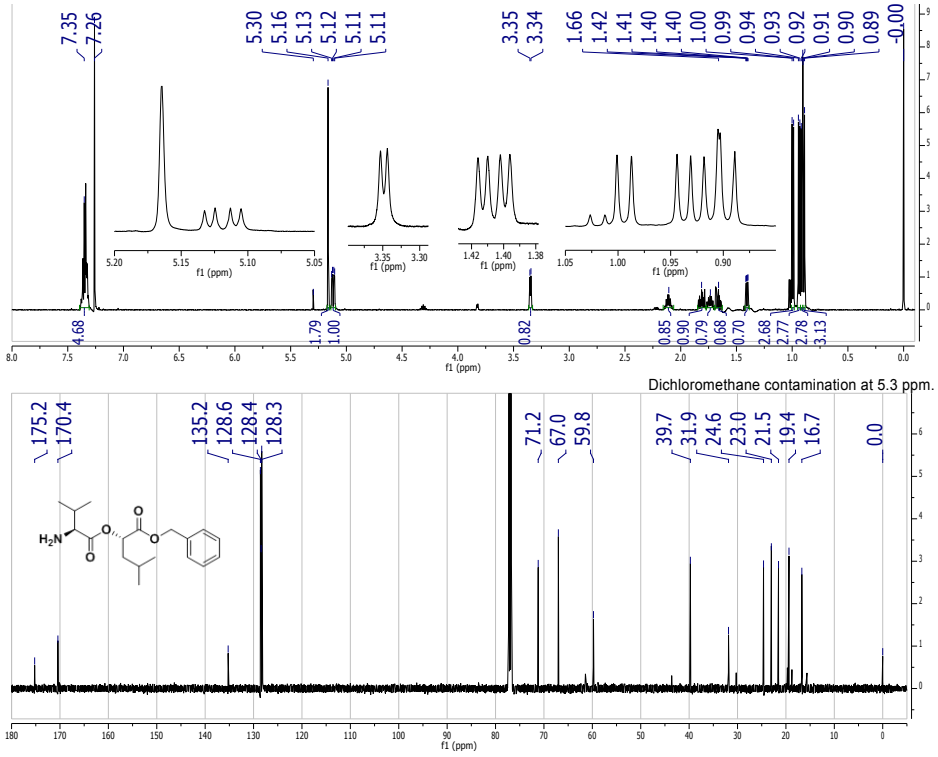

S44. ^{1}H and ^{13}C-NMR spectra of benzyl (*S*)-2-((*L*-phenylalanyl)oxy)-4-methylpentanoate (21c).

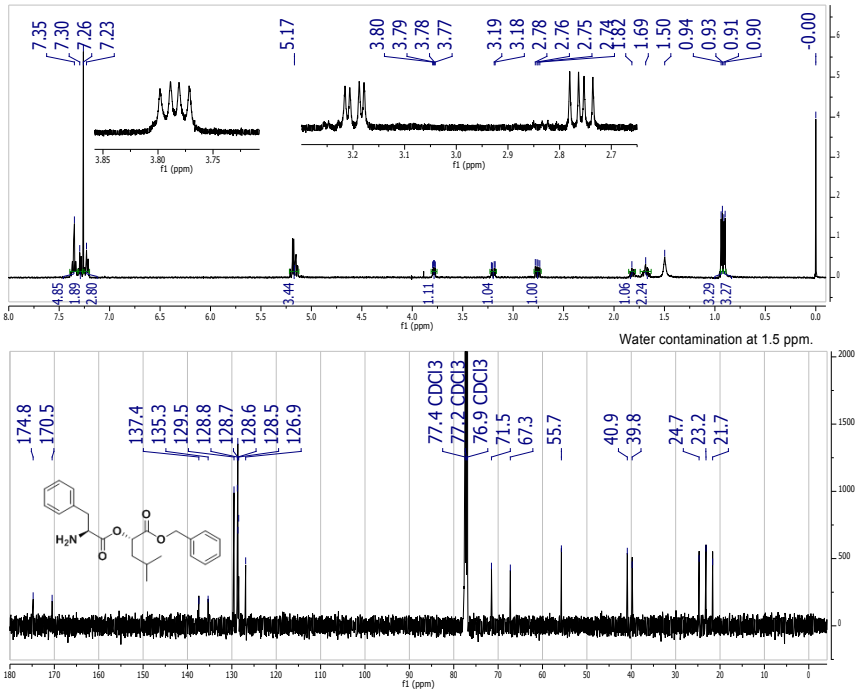

S45. ^{1}H and ^{13}C-NMR spectra of benzyl (*S*)-2-((dimethyl-*L*-isoleucyl)oxy)-4-methylpentanoate (22a).

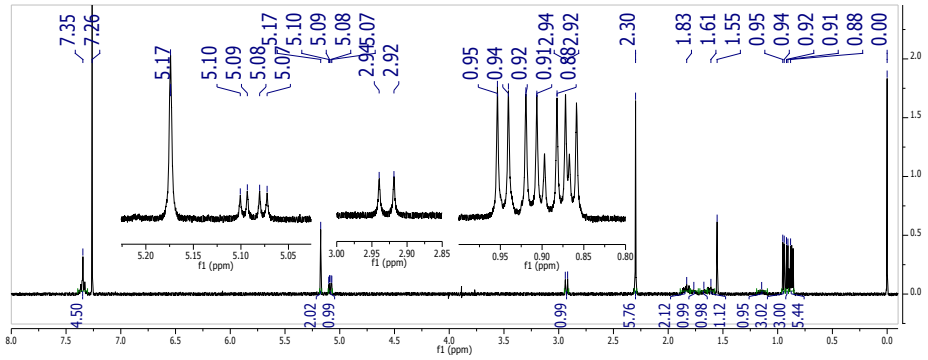

Water contamination at 1.6 ppm.

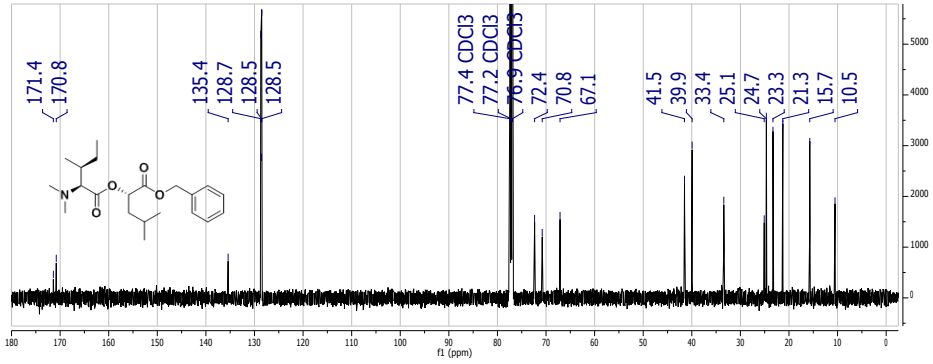

S46. ^{1}H and ^{13}C-NMR spectra of benzyl (*S*)-2-((dimethyl-*L*-valyl)oxy)-4-methylpentanoate (22b).

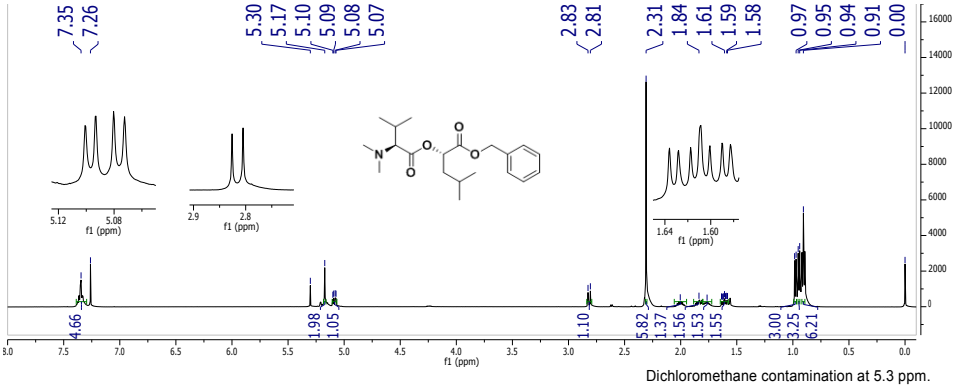

Dichloromethane contamination at 5.3 ppm.

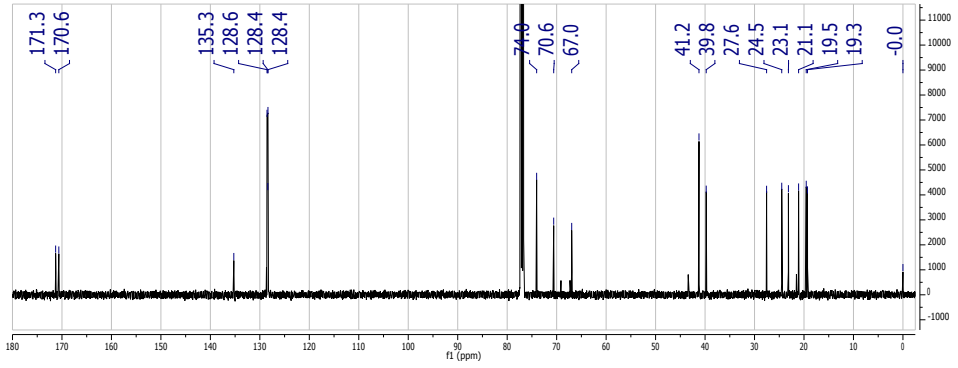

S47. ^{1}H and ^{13}C-NMR spectra of benzyl (*S*)-2-((dimethyl-*L*-phenylalanyl)oxy)-4-methylpentanoate (22c).

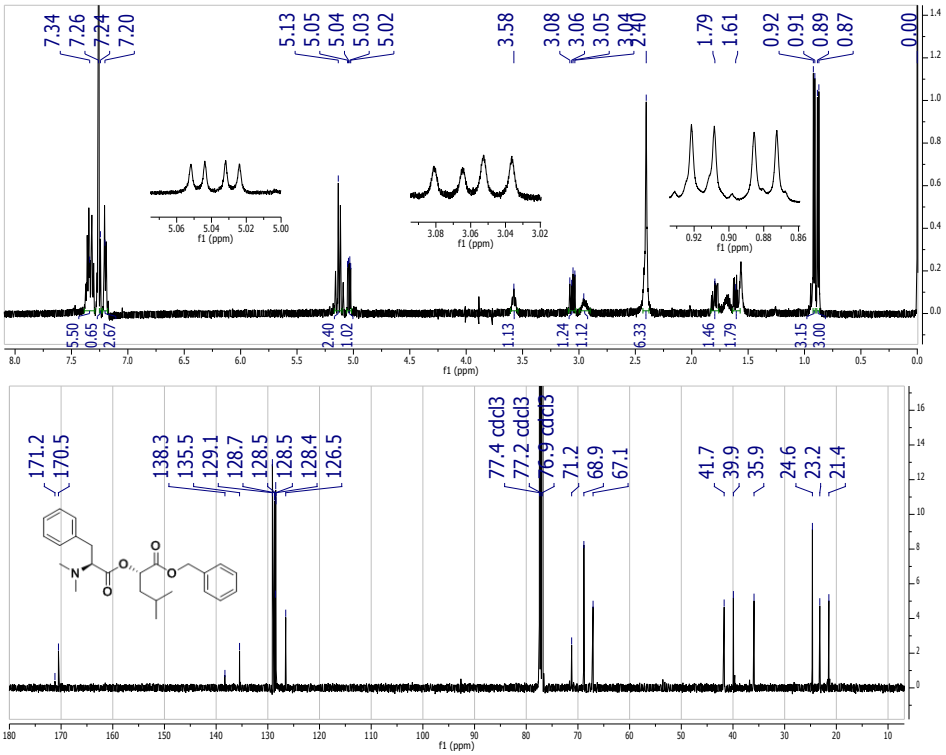

NMR Spectra – Full Products

S48. ^{1}H and ^{13}C-NMR spectra of synthetic gallinamide A (1).

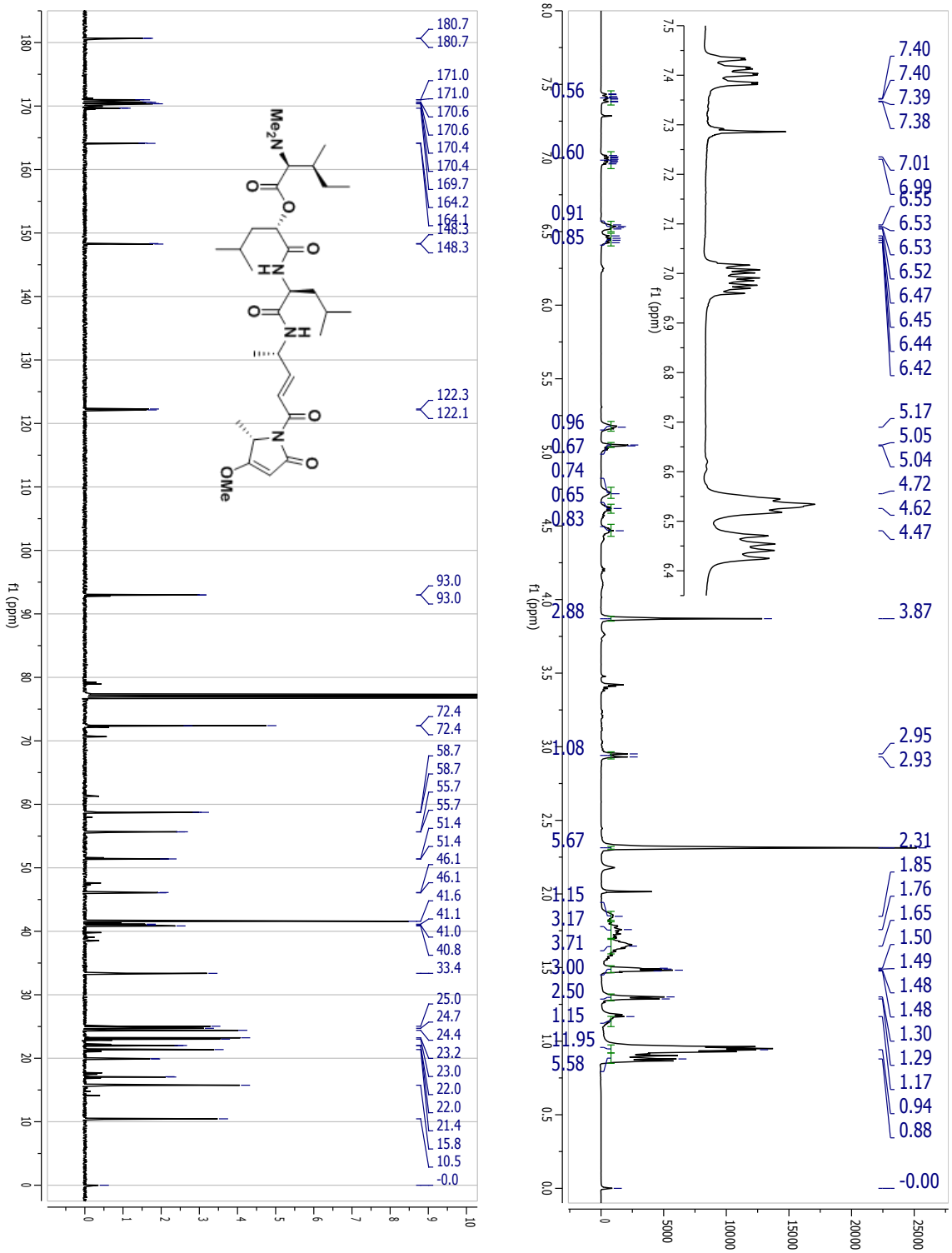

S49. ^{1}H and ^{13}C-NMR spectra of (*S*)-1-(((*S*)-1-(((*S*,*E*)-5-((*S*)-3-methoxy-2-methyl-5-oxo-2,5-dihydro-1*H*-pyrrol-1-yl)-5-oxopent-3-en-2-yl)amino)-4-methyl-1-oxopentan-2-yl)amino)-4-methyl-1-oxopentan-2-yl dimethyl-*L*-valinate (2).

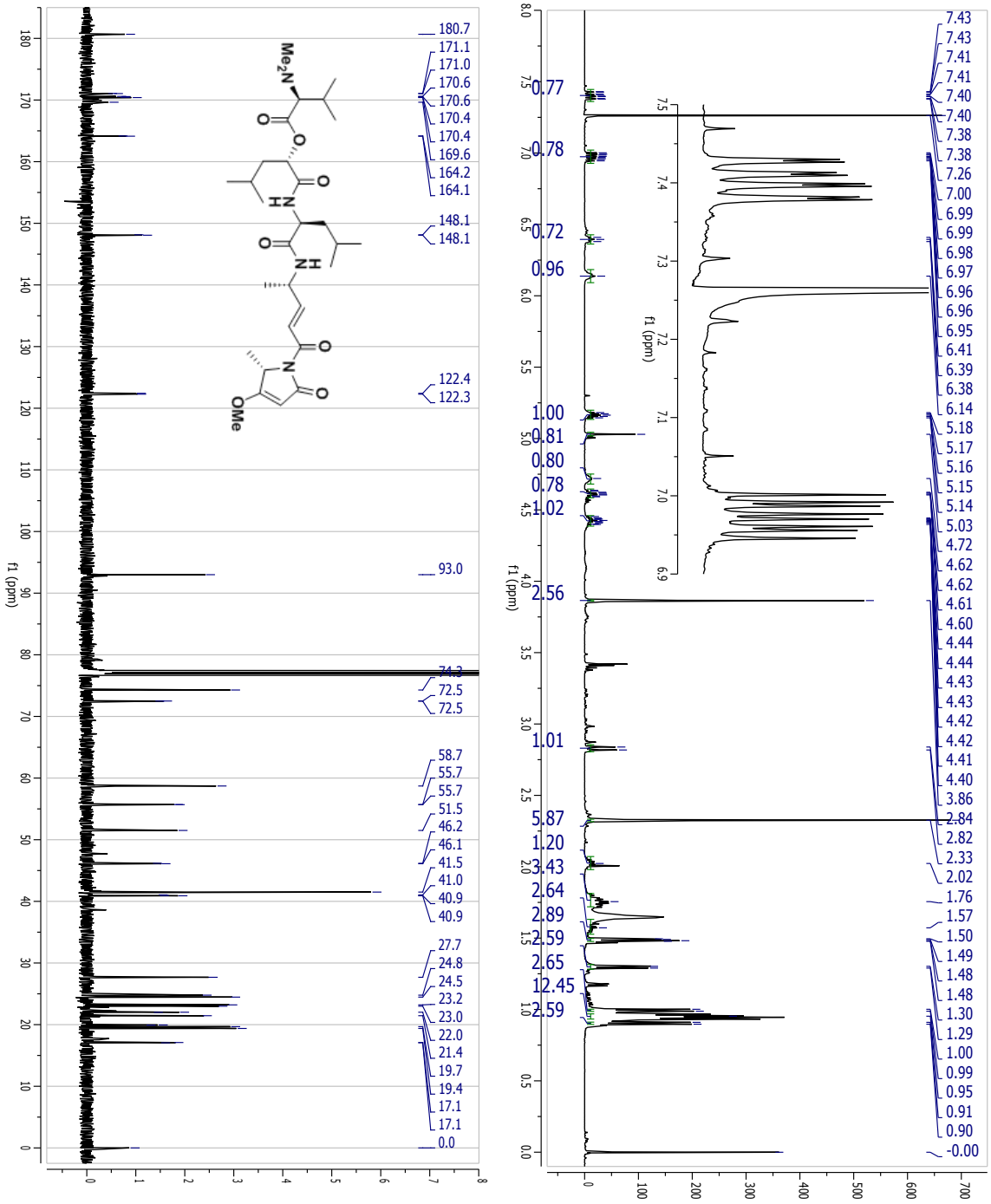

S50. ^{1}H and ^{13}C-NMR spectra of (*S*)-1-(((*S*)-1-(((*S*,*E*)-5-((*S*)-2-benzyl-3-methoxy-5-oxo-2,5-dihydro-1*H*-pyrrol-1-yl)-5-oxopent-3-en-2-yl)amino)-4-methyl-1-oxopentan-2-yl)amino)-4-methyl-1-oxopentan-2-yl dimethyl-*L*-isoleucinate (3).

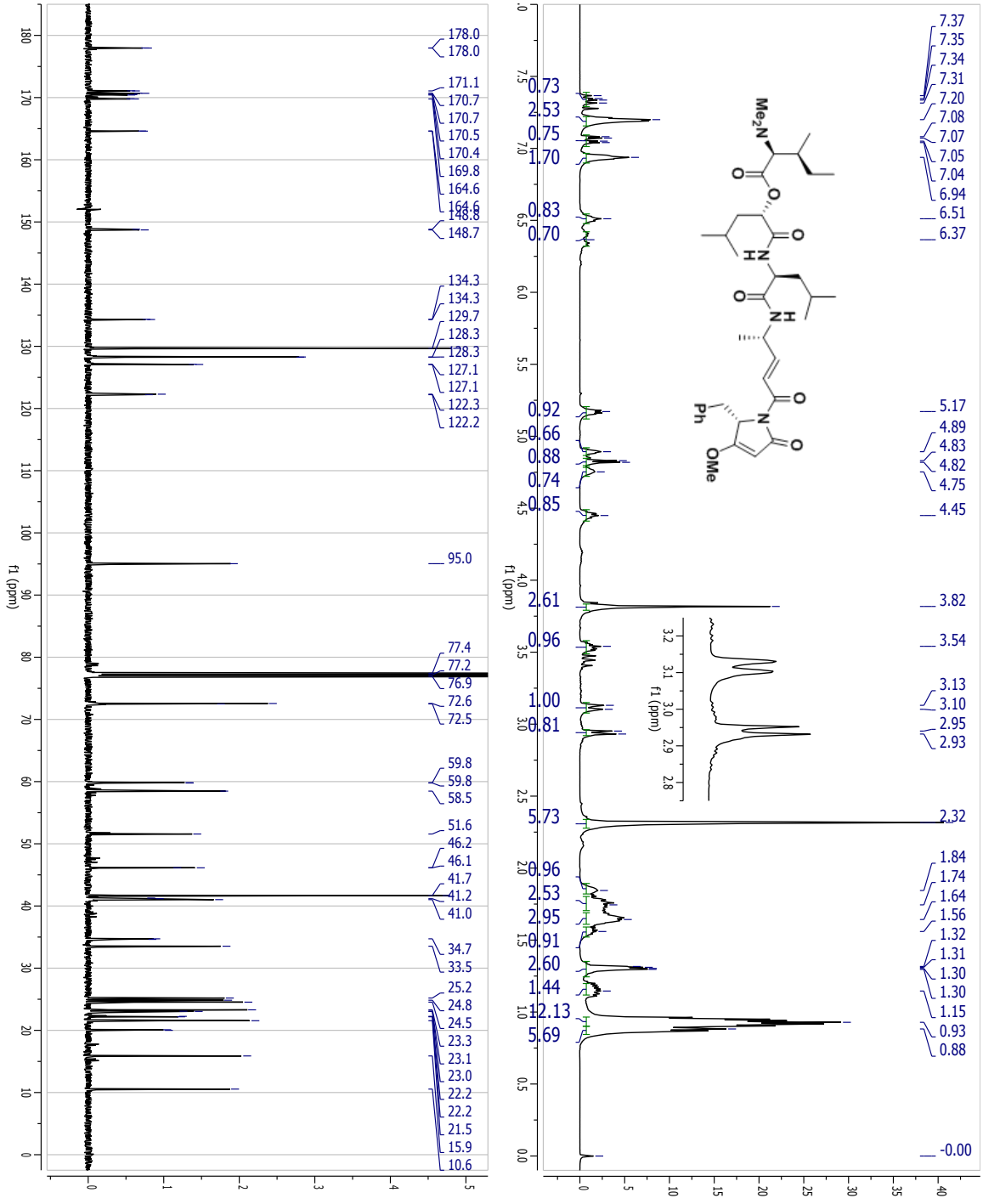

S51. ^{1}H and ^{13}C-NMR spectra of (*S*)-1-(((*S*)-1-(((*S,E*)-5-((*S*)-2-benzyl-3-methoxy-5-oxo-2,5-dihydro-1*H*-pyrrol-1-yl)-5-oxopent-3-en-2-yl)amino)-4-methyl-1-oxopentan-2-yl)amino)-4-methyl-1-oxopentan-2-yl dimethyl-*L*-phenylalaninate (4).

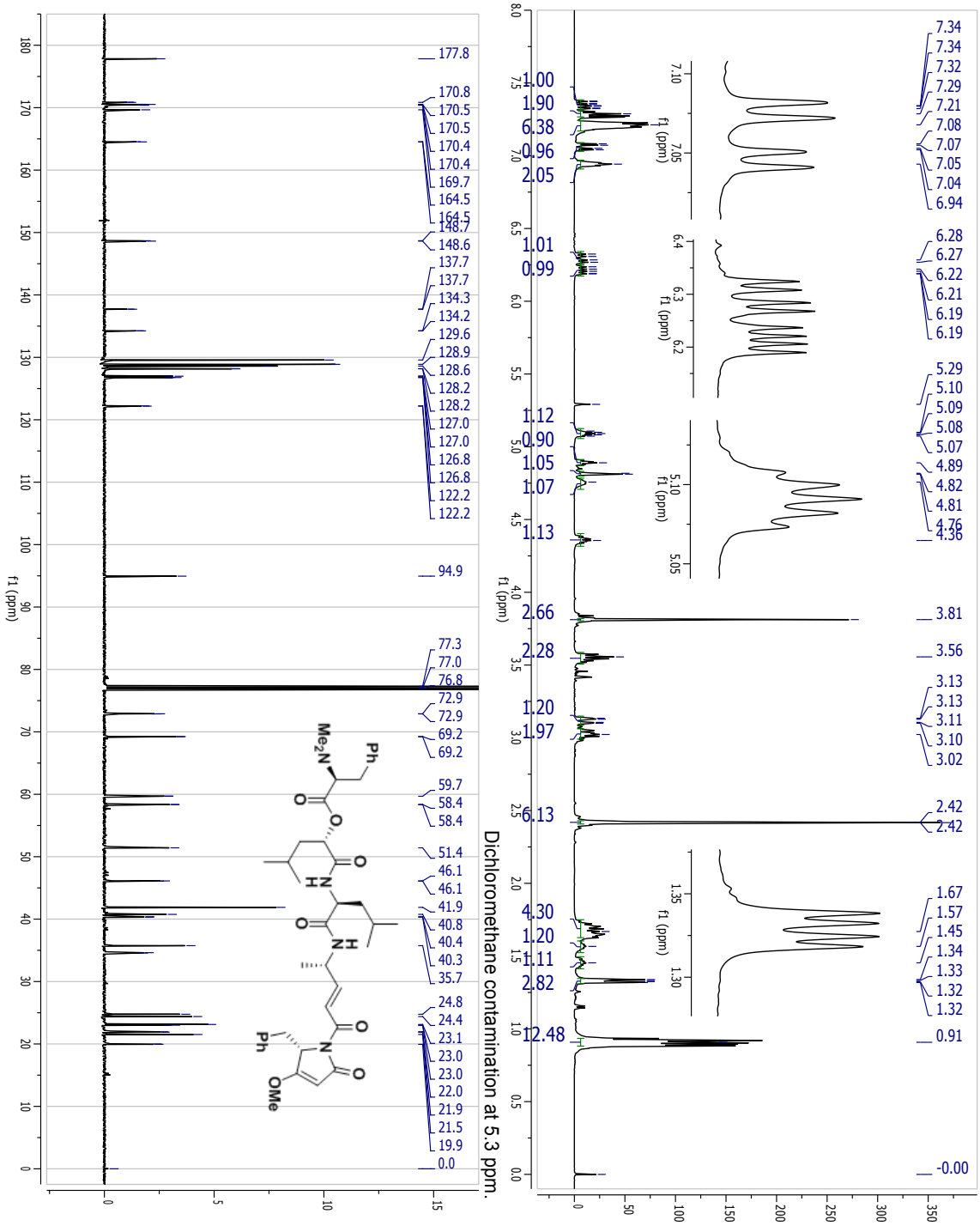

S52. ^{1}H and ^{13}C-NMR spectra of (*S*)-1-(((*S*)-1-(((*S*,*E*)-5-((*S*)-2-isobutyl-3-methoxy-5-oxo-2,5-dihydro-1*H*-pyrrol-1-yl)-5-oxopent-3-en-2-yl)amino)-4-methyl-1-oxopentan-2-yl)amino)-4-methyl-1-oxopentan-2-yl dimethyl-*L*-isoleucinate (5).

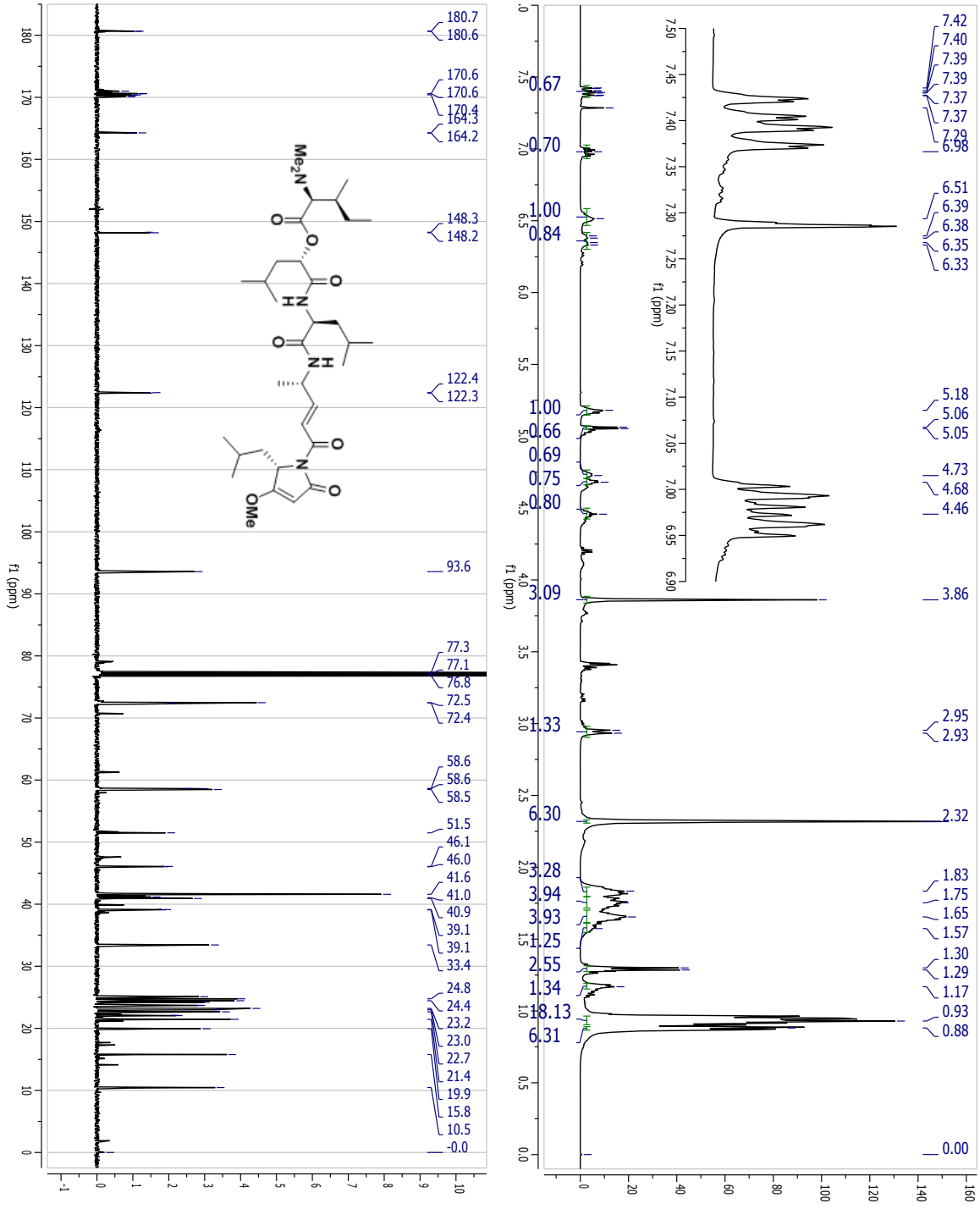

S53. ^{1}H and ^{13}C-NMR spectra of (*S*)-1-(((*S*)-1-(((*S*,*E*)-5-((*S*)-3-methoxy-2-methyl-5-oxo-2,5-dihydro-1*H*-pyrrol-1-yl)-5-oxo-1-phenylpent-3-en-2-yl)amino)-4-methyl-1-oxopentan-2-yl)amino)-4-methyl-1-oxopentan-2-yl dimethyl-*L*-isoleucinate (6).

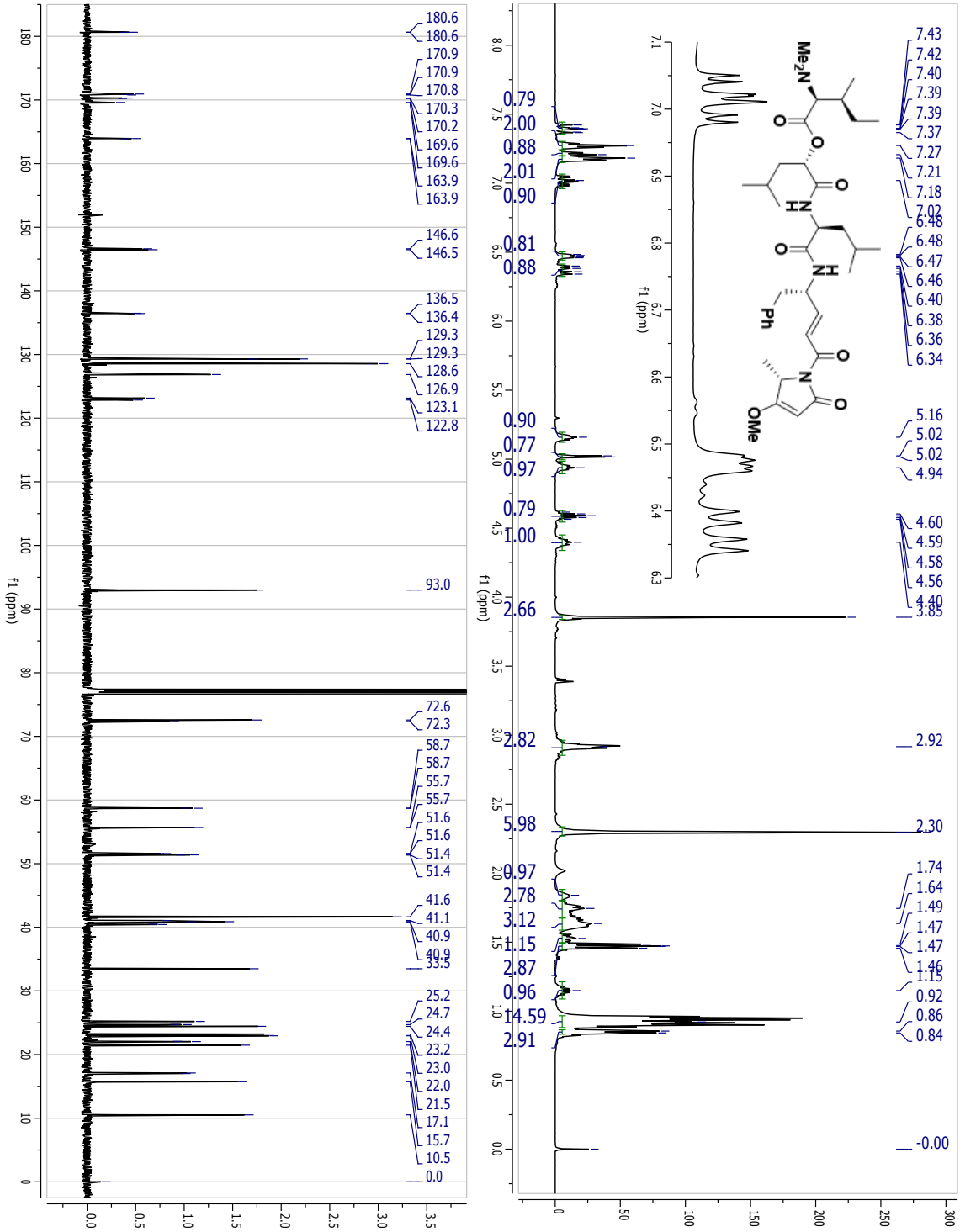

S54. ^{1}H and ^{13}C-NMR spectra of (*S*)-1-(((*S*)-1-(((*S*,*E*)-5-((*S*)-3-methoxy-2-methyl-5-oxo-2,5-dihydro-1*H*-pyrrol-1-yl)-5-oxo-1-phenylpent-3-en-2-yl)amino)-4-methyl-1-oxopentan-2-yl)amino)-4-methyl-1-oxopentan-2-yl dimethyl-*L*-phenylalaninate (7).

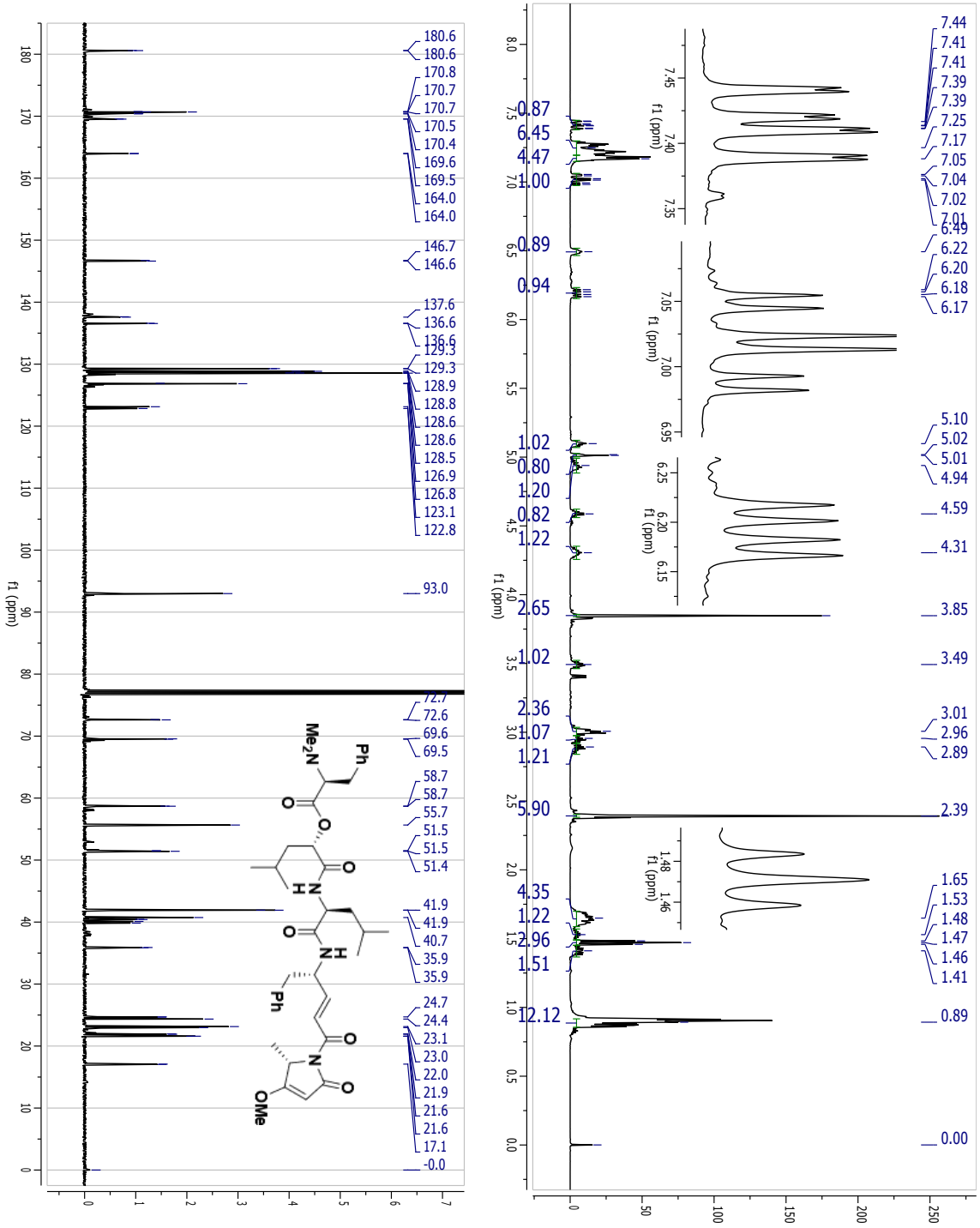

S55. ^{1}H and ^{13}C-NMR spectra of (*S*)-1-(((*S*)-1-(((*S*,*E*)-5-((*S*)-2-benzyl-3-methoxy-5-oxo-2,5-dihydro-1*H*-pyrrol-1-yl)-5-oxo-1-phenylpent-3-en-2-yl)amino)-4-methyl-1-oxopentan-2-yl)amino)-4-methyl-1-oxopentan-2-yl dimethyl-*L*-isoleucinate (8).

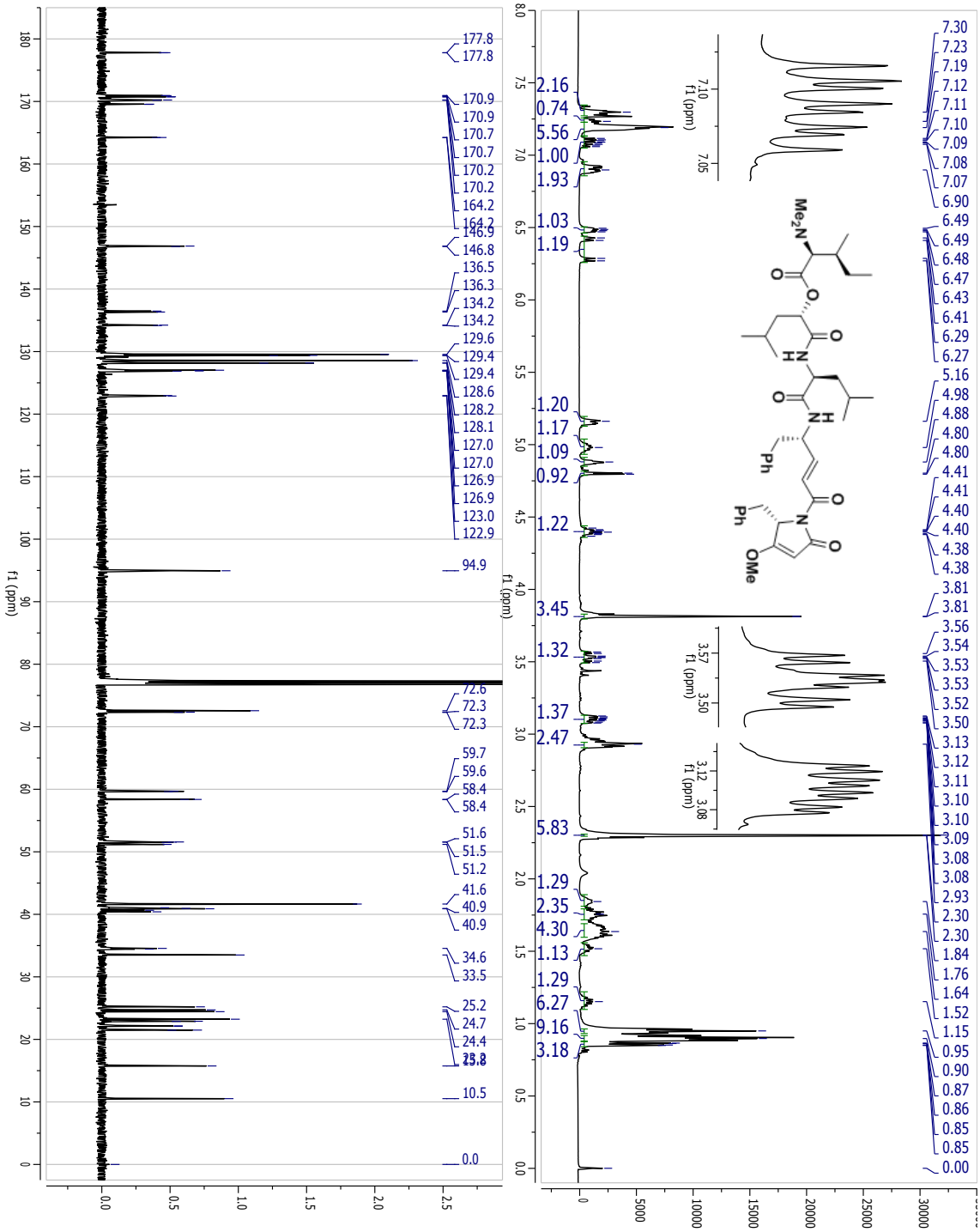

S56. ^{1}H and ^{13}C-NMR spectra of (*S*)-1-(((*S*)-1-(((*S*,*E*)-5-((*S*)-2-benzyl-3-methoxy-5-oxo-2,5-dihydro-1*H*-pyrrol-1-yl)-5-oxo-1-phenylpent-3-en-2-yl)amino)-4-methyl-1-oxopentan-2-yl)amino)-4-methyl-1-oxopentan-2-yl dimethyl-*L*-phenylalaninate (9).

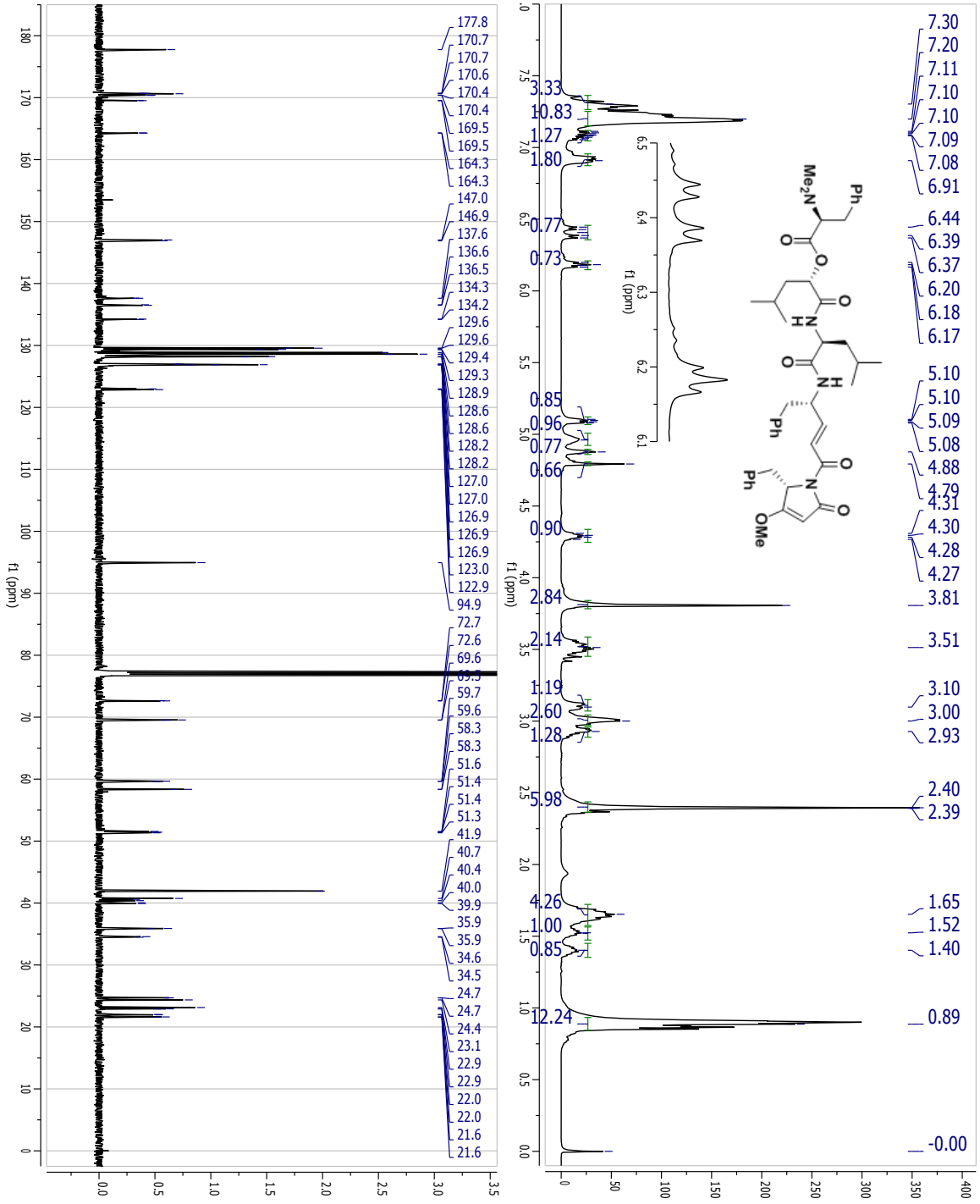

S57. ^{1}H and ^{13}C-NMR spectra of (*S*)-1-(((*S*)-1-(((*S*,*E*)-5-((*S*)-2-isobutyl-3-methoxy-5-oxo-2,5-dihydro-1*H*-pyrrol-1-yl)-5-oxo-1-phenylpent-3-en-2-yl)amino)-4-methyl-1-oxopentan-2-yl)amino)-4-methyl-1-oxopentan-2-yl dimethyl-*L*-isoleucinate (10).

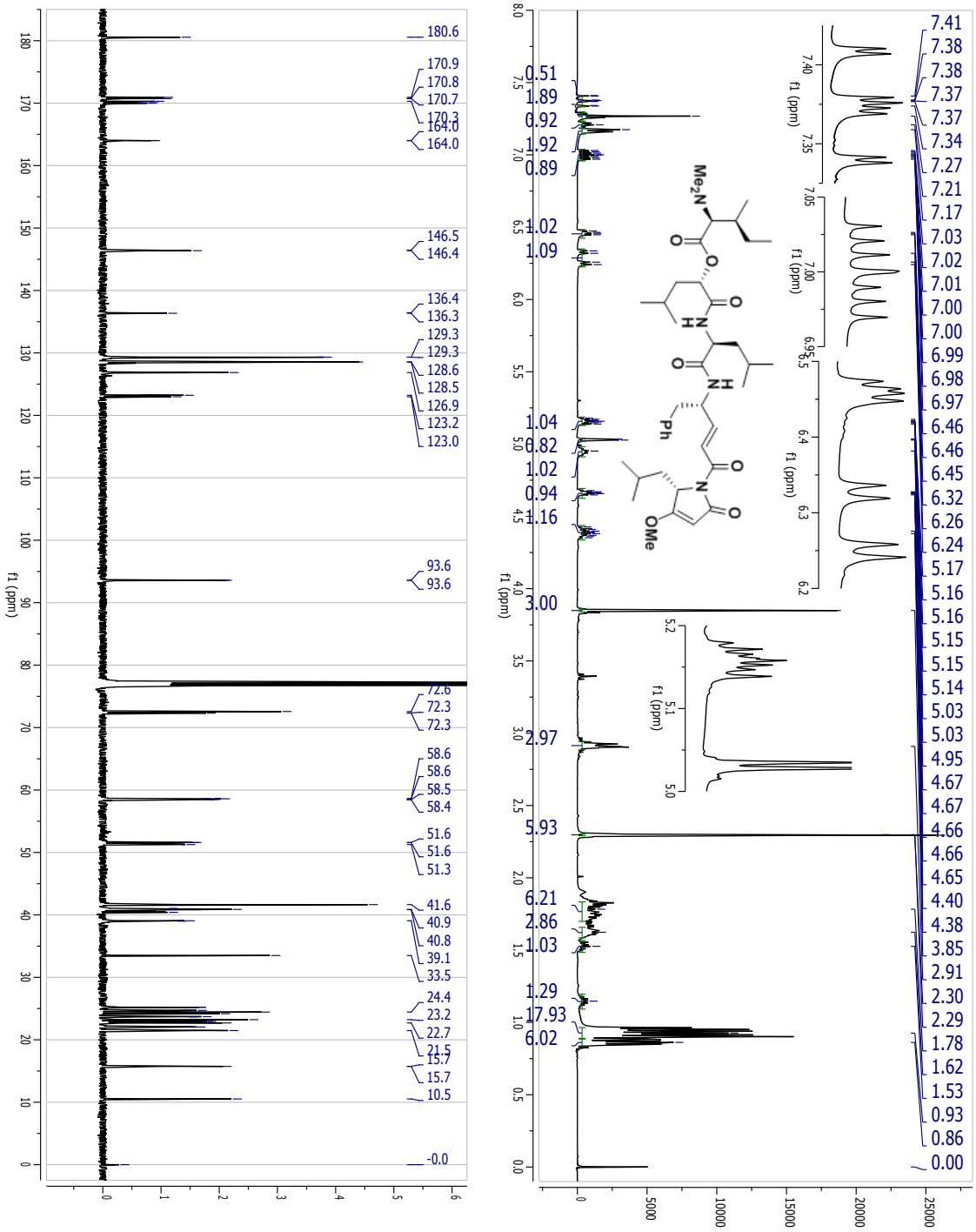

S58. ^{1}H and ^{13}C-NMR spectra of (*S*)-1-(((*S*)-1-(((*S*,*E*)-5-((*S*)-2-isobutyl-3-methoxy-5-oxo-2,5-dihydro-1*H*-pyrrol-1-yl)-5-oxo-1-phenylpent-3-en-2-yl)amino)-4-methyl-1-oxopentan-2-yl)amino)-4-methyl-1-oxopentan-2-yl dimethyl-*L*-valinate (11).

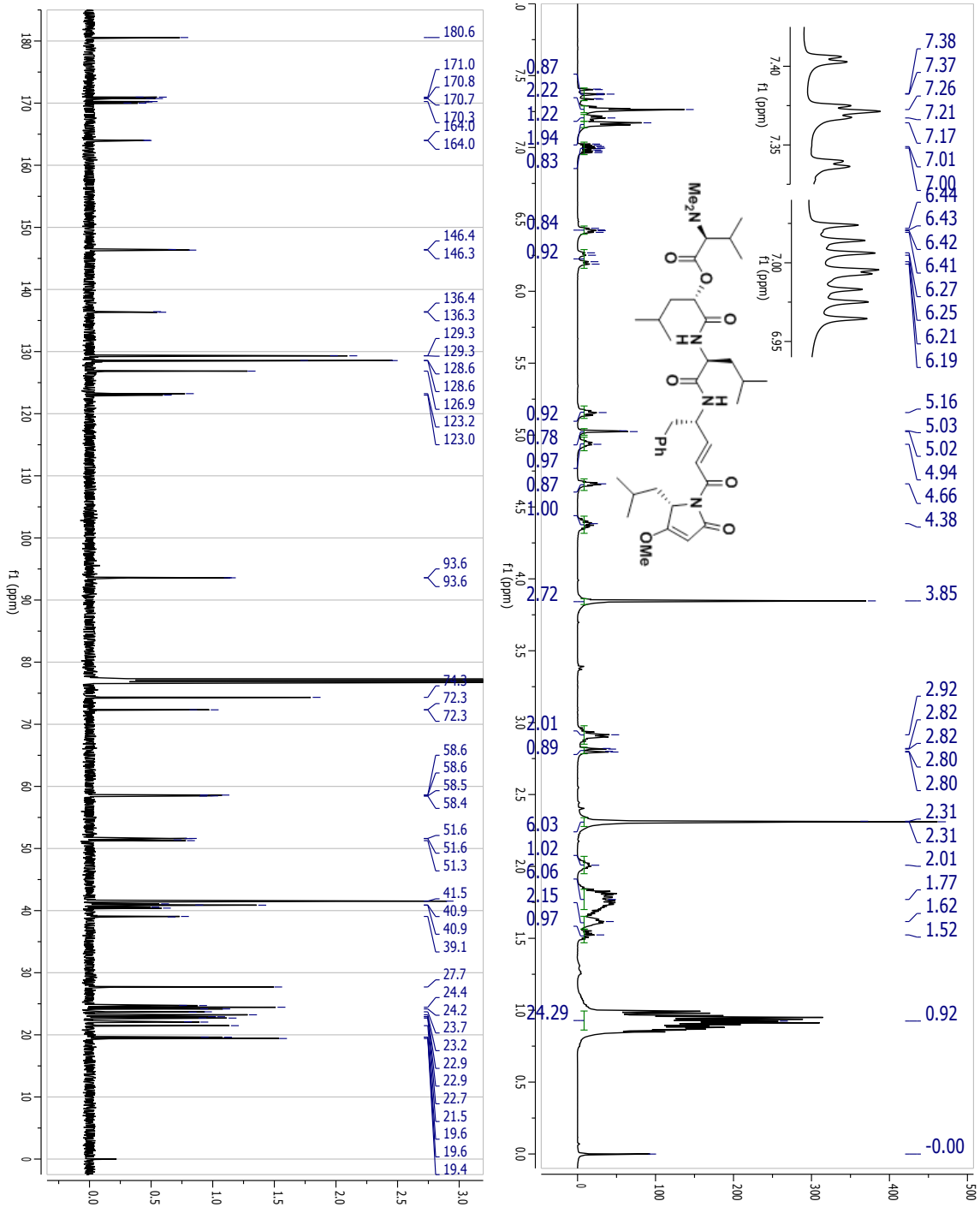

S549 ^{1}H and ^{13}C-NMR spectra of (*S*)-1-(((*S*)-1-(((*S*,*E*)-5-((*R*)-2-benzyl-3-methoxy-5-oxo-2,5-dihydro-1*H*-pyrrol-1-yl)-5-oxo-1-phenylpent-3-en-2-yl)amino)-4-methyl-1-oxopentan-2-yl)amino)-4-methyl-1-oxopentan-2-yl dimethyl-*L*-isoleucinate (12).

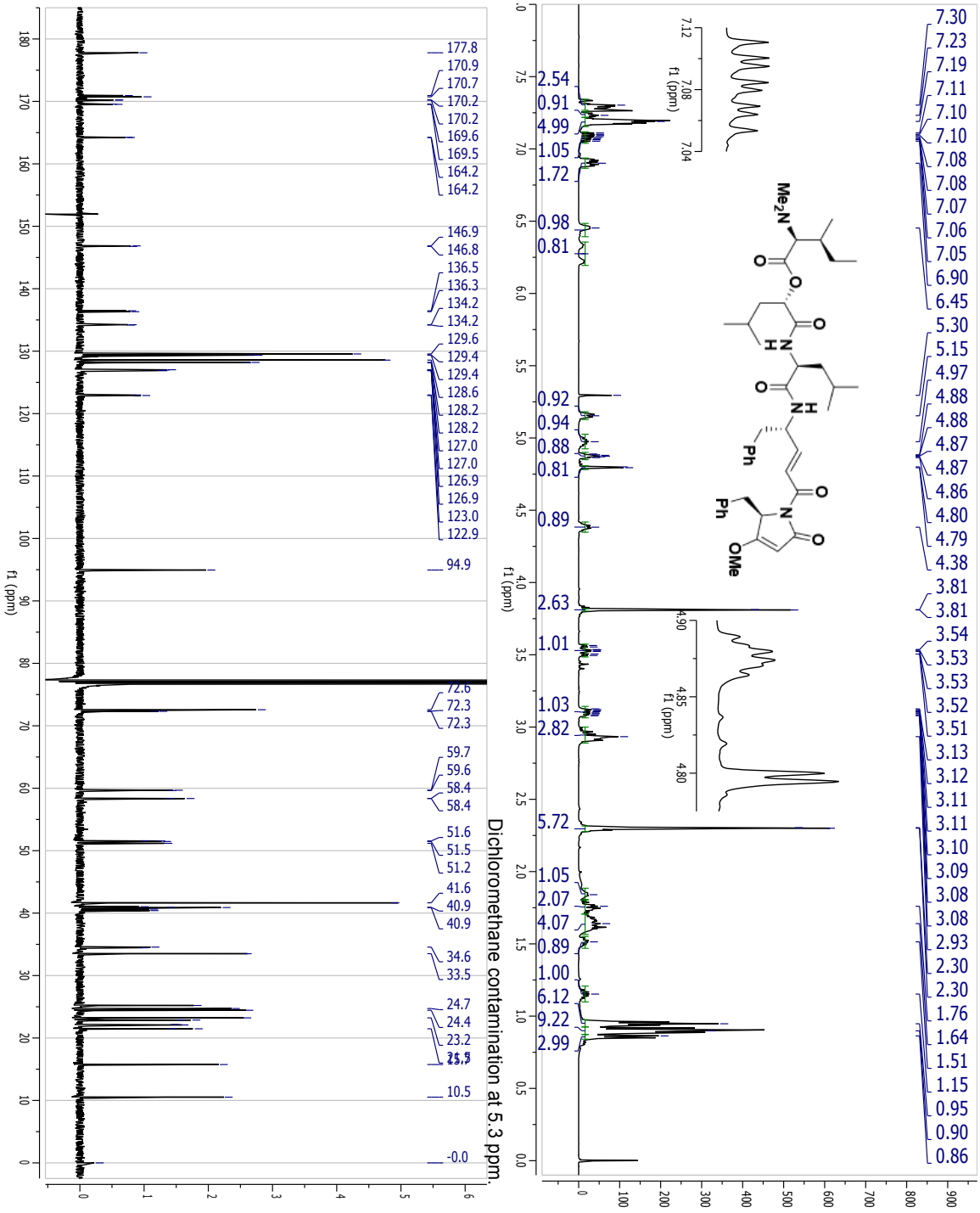

S60. ^{1}H and ^{13}C-NMR spectra of (*S*)-1-(((*S*)-1-(((*S*,*E*)-5-((*R*)-2-benzyl-3-methoxy-5-oxo-2,5-dihydro-1*H*-pyrrol-1-yl)-5-oxo-1-phenylpent-3-en-2-yl)amino)-4-methyl-1-oxopentan-2-yl)amino)-4-methyl-1-oxopentan-2-yl dimethyl-*L*-phenylalinate (13).

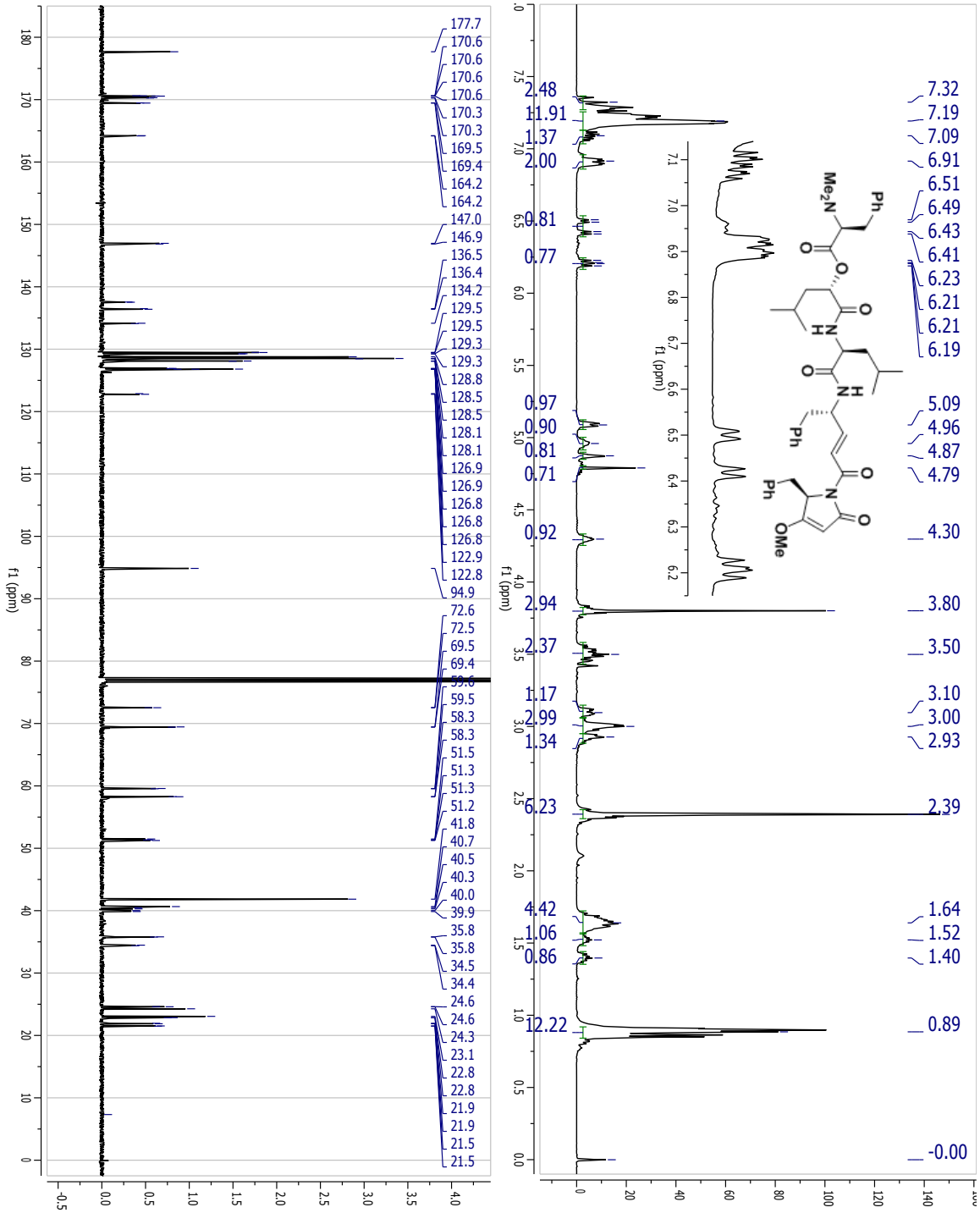

S61. ^{1}H and ^{13}C-NMR spectra of (*S*)-1-(((*S*)-1-(((*R*,*E*)-5-((*S*)-2-benzyl-3-methoxy-5-oxo-2,5-dihydro-1*H*-pyrrol-1-yl)-5-oxo-1-phenylpent-3-en-2-yl)amino)-4-methyl-1-oxopentan-2-yl)amino)-4-methyl-1-oxopentan-2-yl dimethyl-*L*-isoleucinate (14).

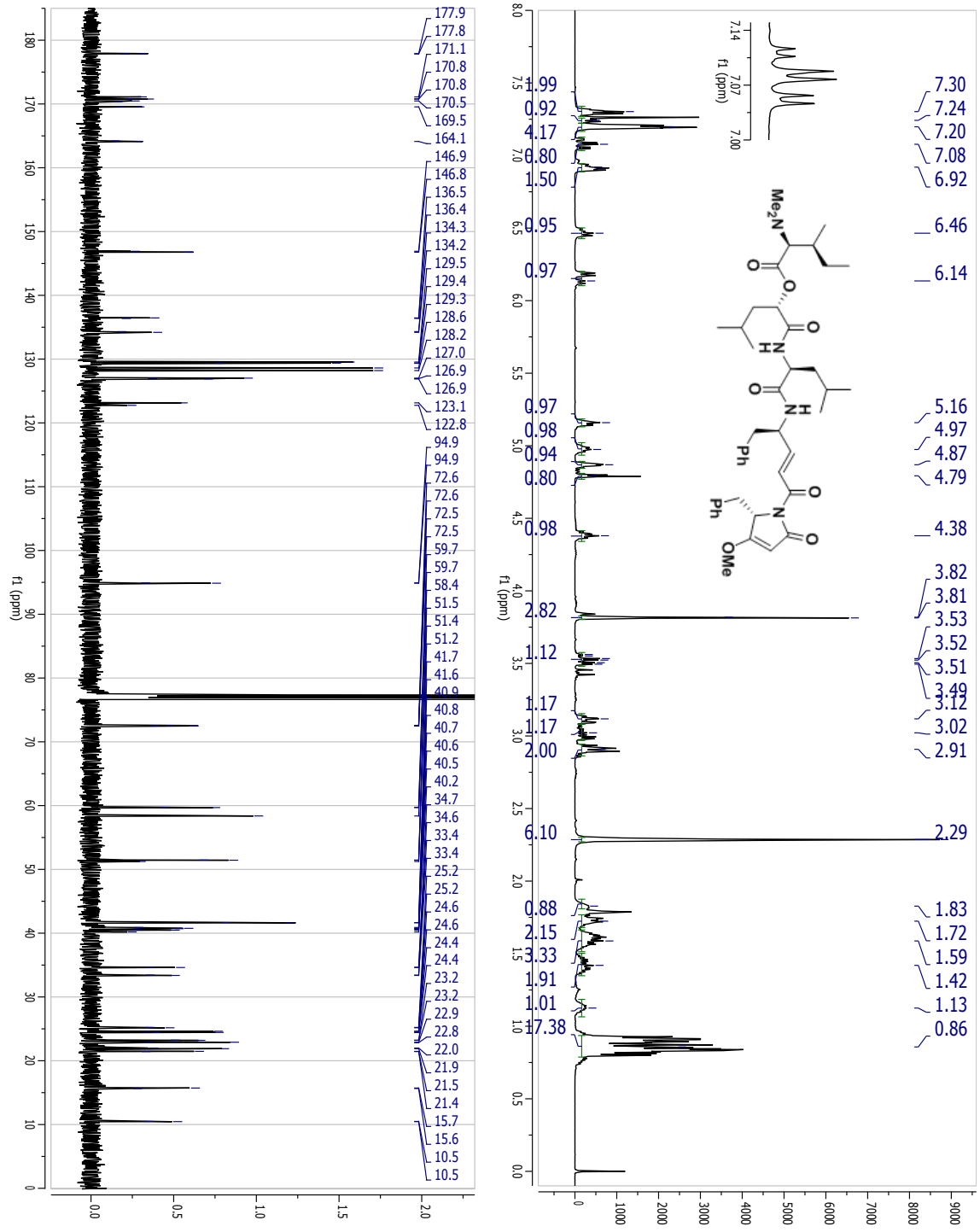

S62. ^{1}H and ^{13}C-NMR spectra of (*S*)-1-(((*S*)-1-(((*R*,*E*)-5-((*R*)-2-benzyl-3-methoxy-5-oxo-2,5-dihydro-1*H*-pyrrol-1-yl)-5-oxo-1-phenylpent-3-en-2-yl)amino)-4-methyl-1-oxopentan-2-yl)amino)-4-methyl-1-oxopentan-2-yl dimethyl-*L*-isoleucinate (15).

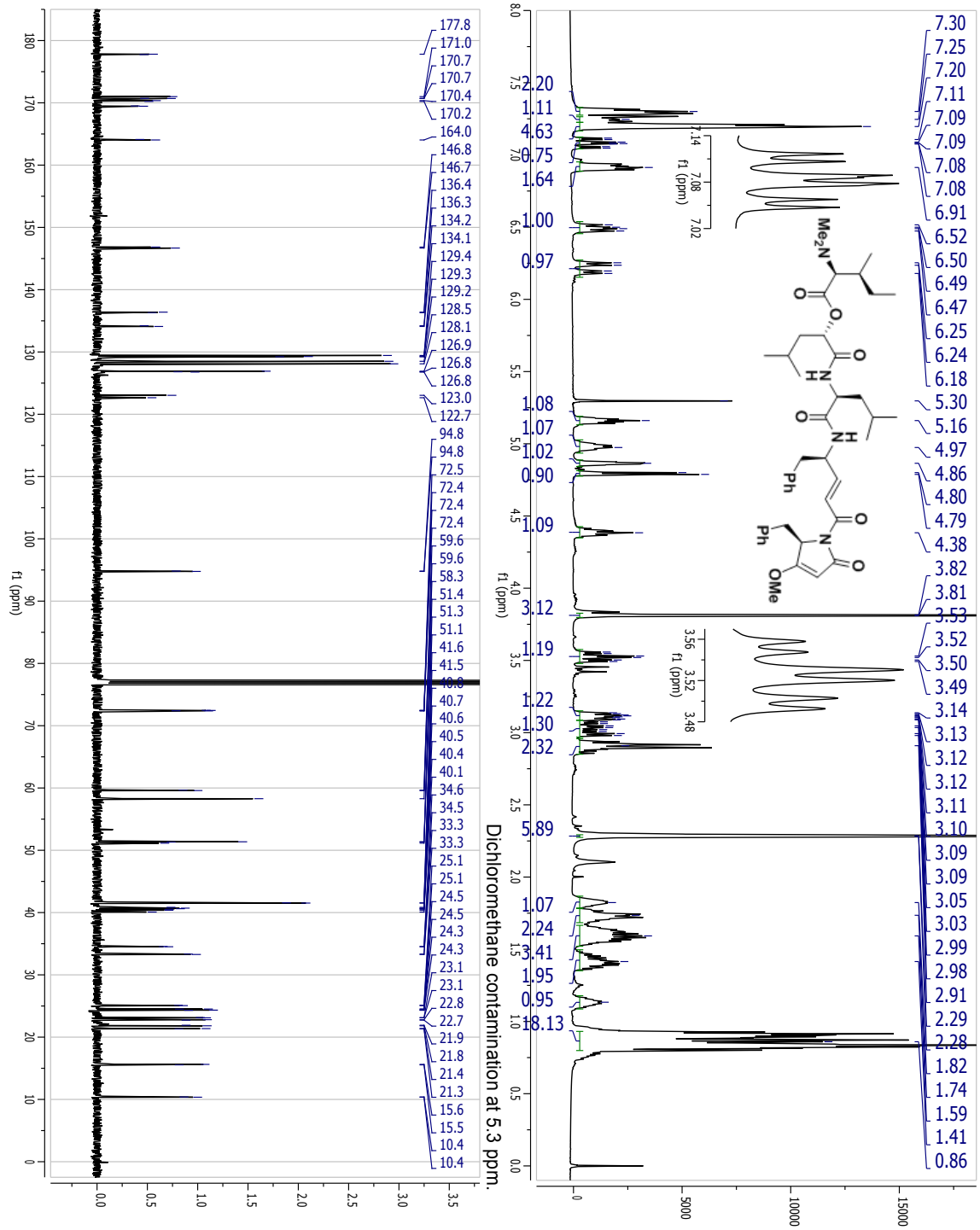

S63. ^{1}H and ^{13}C-NMR spectra of (*S*)-1-(((*S*)-1-(((*S*,*E*)-5-((*S*)-3-(hex-5-yn-1-yloxy)-2-methyl-5-oxo-2,5-dihydro-1*H*-pyrrol-1-yl)-5-oxopent-3-en-2-yl)amino)-4-methyl-1-oxopentan-2-yl)amino)-4-methyl-1-oxopentan-2-yl dimethyl-*L*-isoleucinate (16).

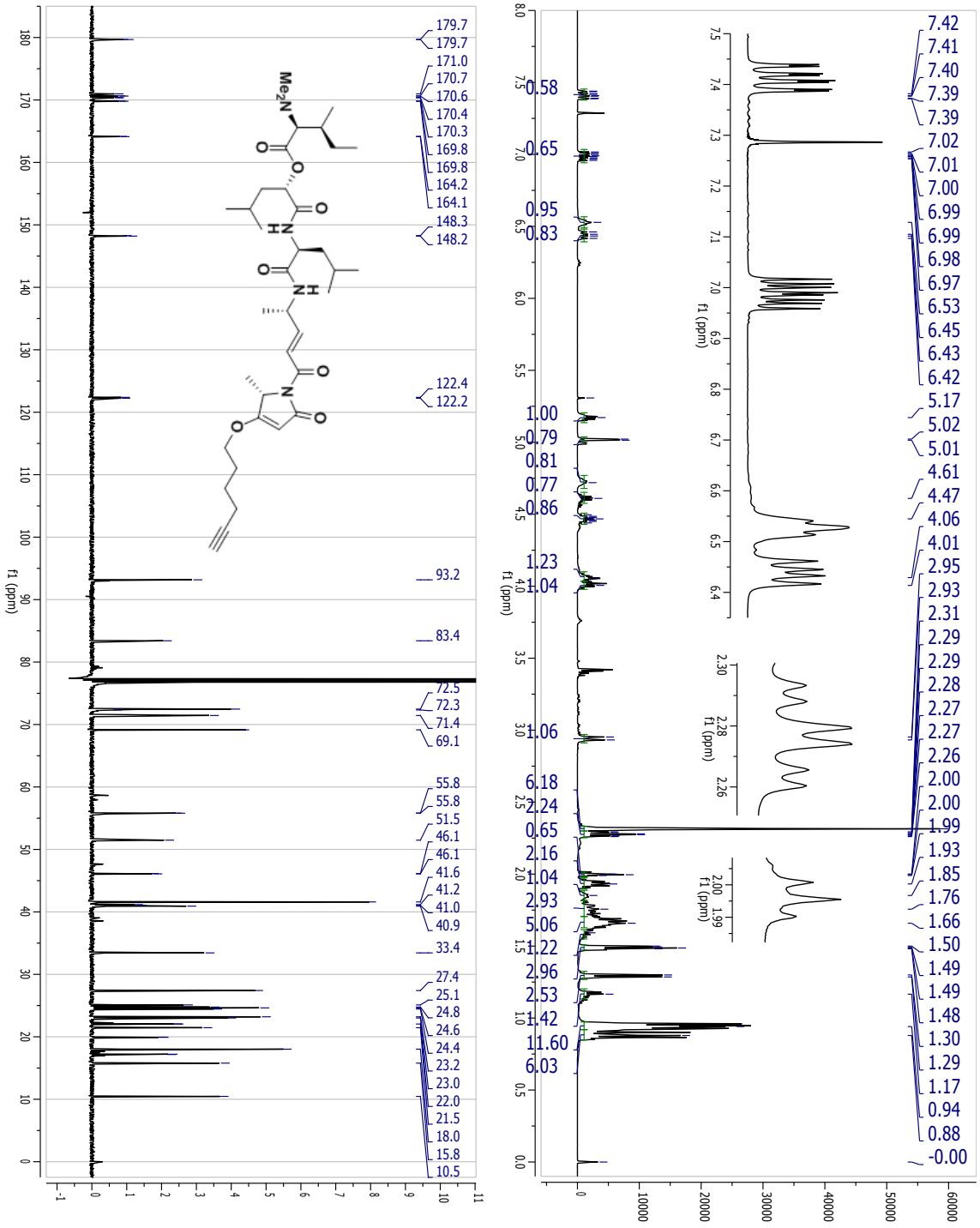

S64. ^{1}H and ^{13}C-NMR spectra of (*S*)-1-(((*S*)-1-(((*S*)-5-((*S*)-3-methoxy-2-methyl-5-oxo-2,5-dihydro-1*H*-pyrrol-1-yl)-5-oxopentan-2-yl)amino)-4-methyl-1-oxopentan-2-yl)amino)-4-methyl-1-oxopentan-2-yl dimethyl-*L*-isoleucinate (17).

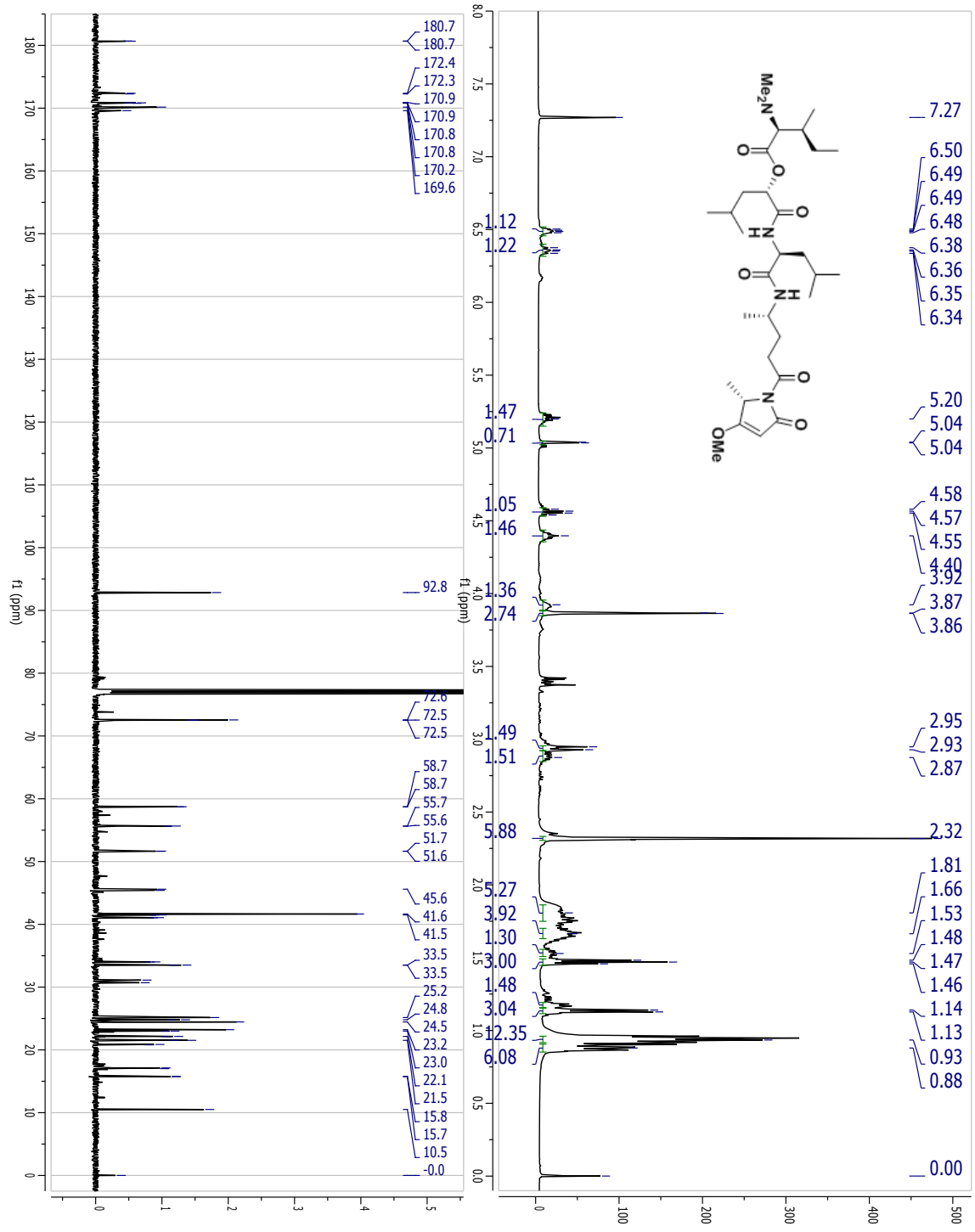

S65. NMR signal splitting and variable temperature experiments.

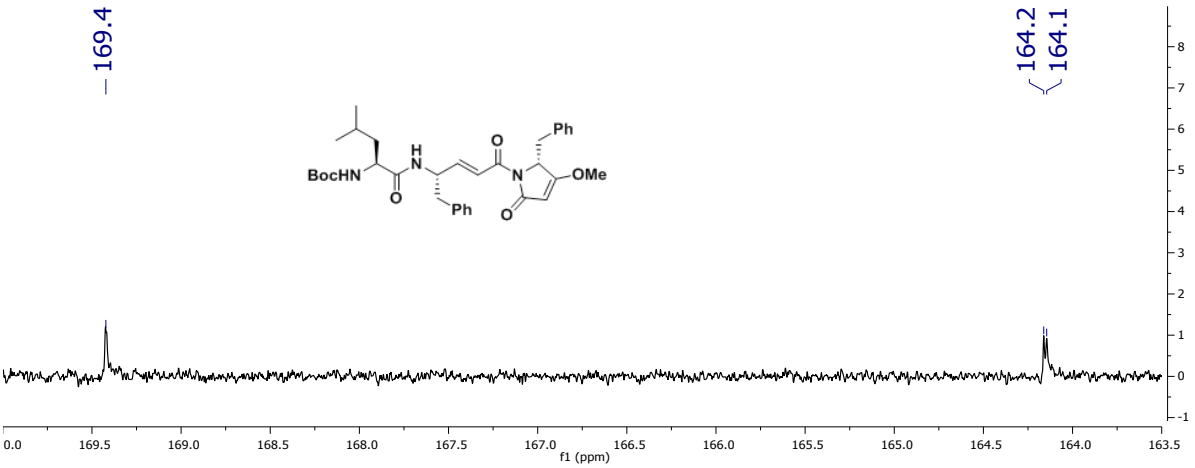

After completing the Mitsunobu reaction, intermediates demonstrated split signals for some NMR signals, seen here in one of the carbonyl carbon signals for intermediate **25g** (*above*). This result could be explained by racemization of a stereocenter during the reaction, or the presence of amide rotamers. A variable temperature NMR experiment with the same intermediate showed convergence of some peaks in the proton spectrum, visible in the alkene proton the enamide alkene and the methyl group of the enol ether (*below*), which we believe suggests an issue of amide rotamers across the carbon nitrogen bond connecting the headgroup to the enamide core.

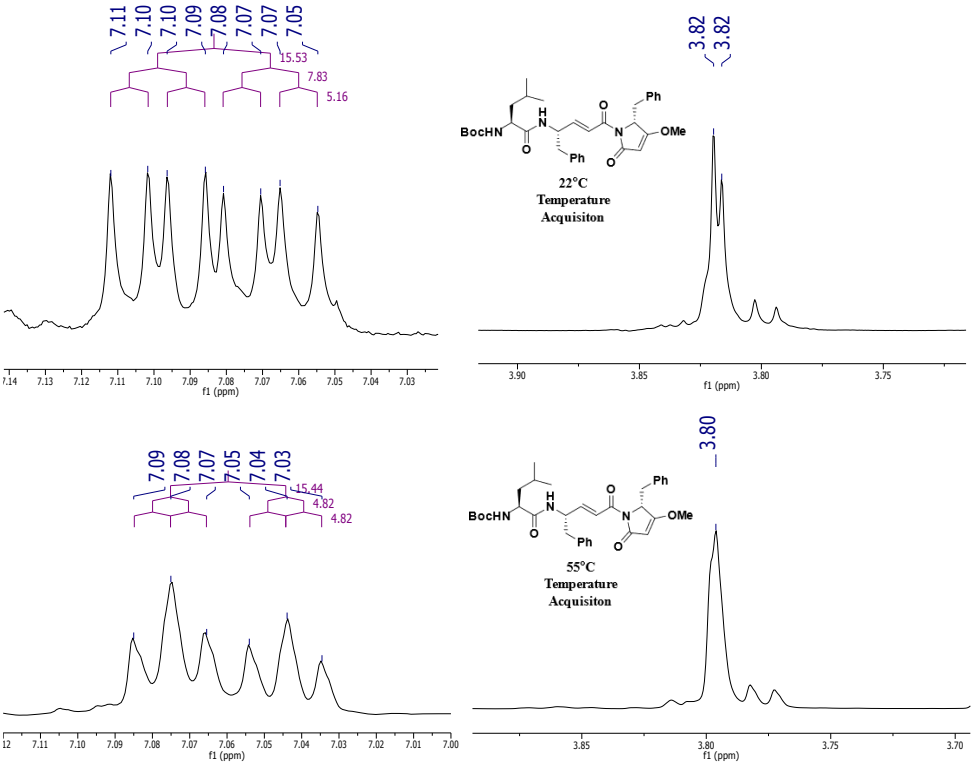

S66. Marfey's analysis results.

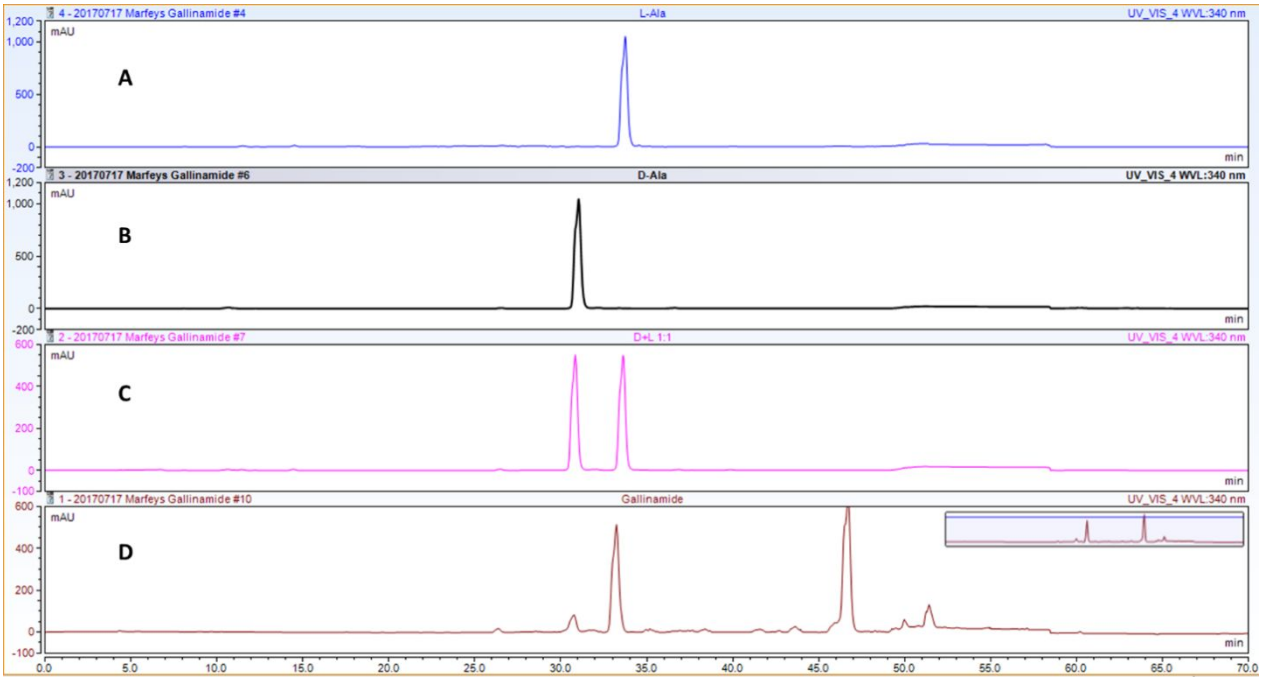

Figure S61. HPLC analysis of the commercially available amino acid standards of L-alanine (**A**), D-alanine (**B**), 1:1 mixture of L-alanine and D-alanine (**C**), and synthetic gallinamide A, compound **1** (**D**), after ozonolysis, hydrolysis and derivatization with 1-fluoro-2-4-dinitrophenyl-5-L-alanine amide (FDAA) at 340 nm.

S67. Gaussian modeling results.

A model compound (**A**) was designed in GaussView 6.0.16 and the dihedral angle of atoms of the four atoms indicated in the figure was set manually at 0, 90, 180, and 270 degrees. The geometry of these structures was energy minimized with Gaussian '09 using the PDDG method with chloroform modeled by SCRF with a polarizable continuum model. The outputs of these optimizations were then used as the initial orientation for a potential energy scan, this time using the B3LYP method with the 6-31+G(d) basis set. The dihedral angle of the four atoms indicated was rotated for at least 71 increments of 5 degrees. If the scan did not arrive at a similar energy when the angle returned to the original orientation the scan was rejected and repeated beginning from the minimal energy value observed in the scan (**B**). Finally, the differences between the absolute minimum at around 195 degrees and local maxima at around 295 degrees were compared to calculate the barrier to rotation (**C**). The resulting barriers were 13.5, 12.2, and 12.9 kcal/mol with a standard deviation of 0.7 kcal/mol. (**D**) Depiction of the interconversion of the two tertiary amide rotomers connecting the Apa unit to the pyrrolidone ring.

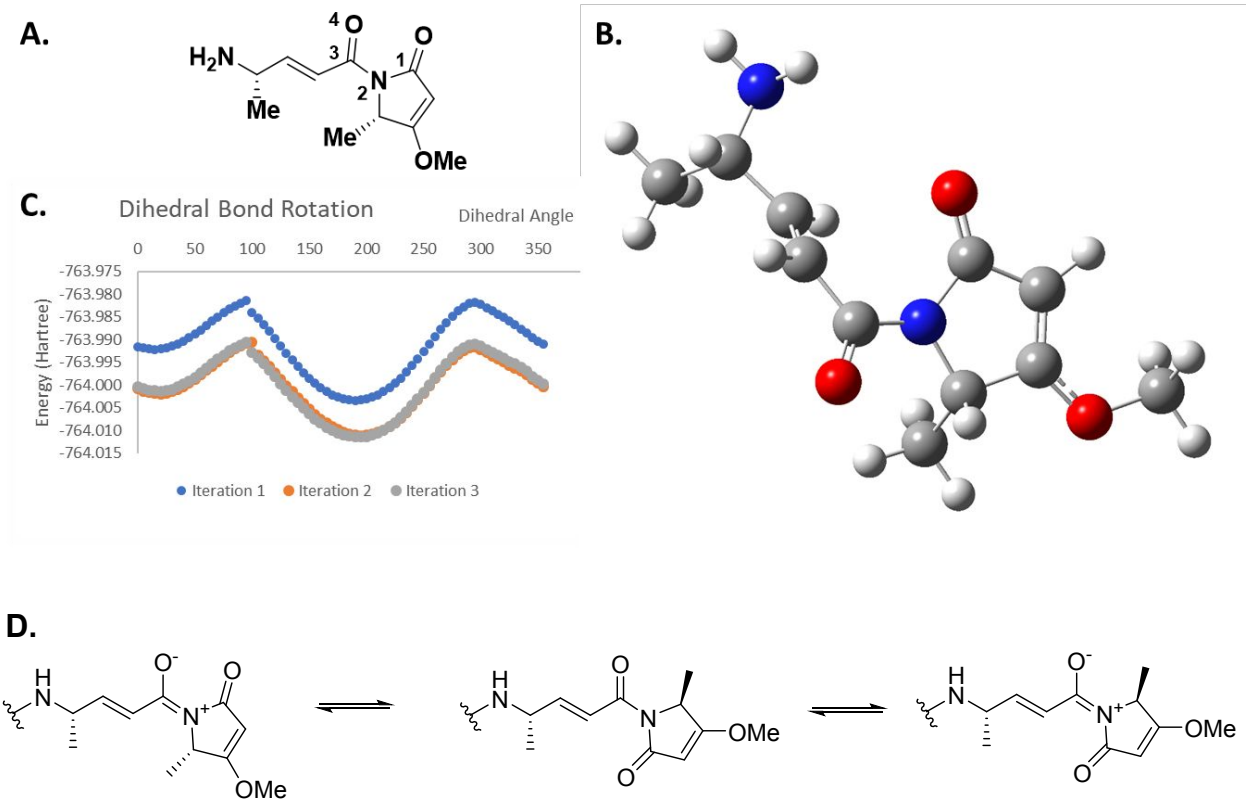

S68. Summary table of calculated kinetic parameters.

Analog	k.aS	k.dS	k.cat	k.aI	k.dI	k.inact	k.I (nM)	k.inact/k.I
1	20	1	75.9	200	0.829	0.00538	4.67 ± 0.40	901000
2	20	1	72.9	200	0.271	0.00463	1.35 ± 0.088	3480000
3	20	1	84.1	200	0.345	0.00429	1.73 ± 0.14	2510000
4	20	1	95.9	200	0.934	0.00416	4.15 ± 0.24	1300000
5	20	1	92.2	200	1.328	0.00319	6.64 ± 0.44	487000
6	20	1	124.5	200	0.158	0.00283	0.791 ± 0.049	3600000
7	20	1	110.1	200	0.706	0.00272	3.53 ± 0.22	818000
8	20	1	166.3	200	0.708	0.00284	3.54 ± 0.22	819000
9	20	1	97.3	200	0.336	0.00171	1.68 ± 0.13	1030000
10	20	1	123.0	200	0.200	0.00132	1.00 ± 0.15	1390000
11	20	1	197.0	200	0.625	0.00232	3.13 ± 0.34	719000
12	20	1	100.2	200	0.262	0.00124	1.31 ± 0.39	1060000
13	20	1	76.2	200	75.100	0.00259	376 ± 25	6900
14	20	1	87.1	200	15.400	0.00181	77 ± 6.6	23900
15	20	1	70.0	200	0.017	0.00085	0.0937 ± 0.010	8730000
16	20	1	630.0	200	0.119	0.00113	0.632 ± 0.035	1780000

Kinetic constants calculated for each gallinamide analog. k.aS, k.dS, and k.aI were fixed at 19, 1, and 200, respectively. k.cat, k.dI, and k.inact were explicitly calculated by DynaFit, and figures in this table represent mean values of triplicate plate experiments, each with triplicate wells for each concentration. k.I and k.inact/k.I are calculated as described in the methods.

S69. Modeled binding of gallinamide A (1) to cruzain.

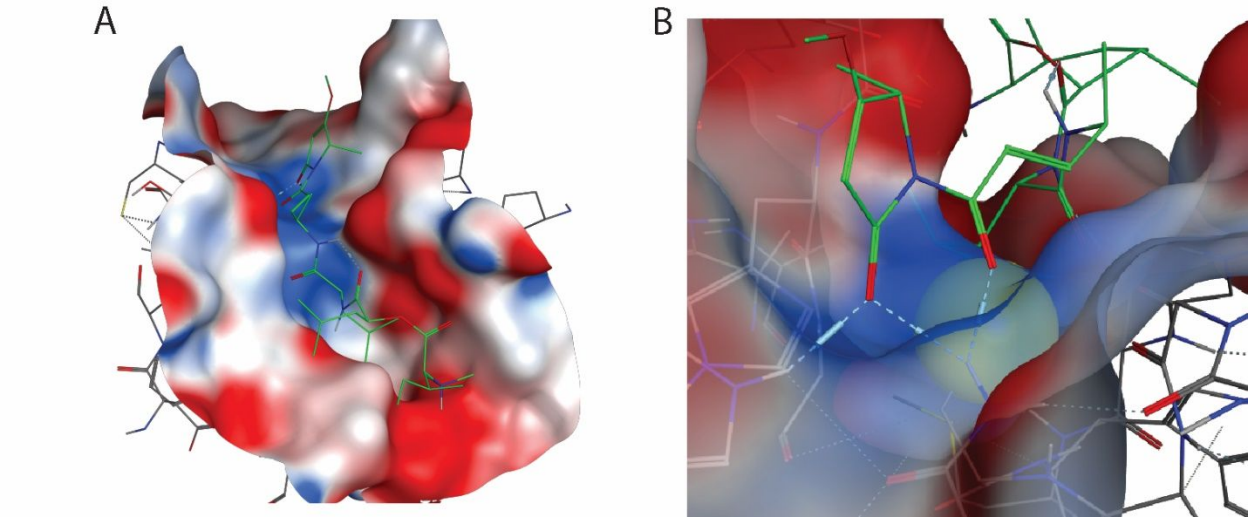

A.) Gallinamide A docked in the active site cleft of cruzain. The lowest energy docking pose of the compound is very similar to that in human cathepsin L.
B.) The hydrogen bond network in the oxyanion hole of the cruzain binding pocket is almost identical to that of cathepsin L.

S70. HPLC purity determination for gallinamide analogues 2-5

LCMS data for purity analysis of the synthesized compounds **2**−**17** were obtained with a Thermo Finnigan Surveyor Autosampler-Plus/LC-Pump-Plus/PDA-Plus system and a Thermo Finnigan LCQ Advantage Max mass spectrometer (5µ C18 Kinetex 100 x 4.6 mm, monitoring 200−600 nm and *m/z* 150−2000 in positive ion mode) using a linear gradient of 30 -100% H_2O/acetonitrile over 14 min; flow rate of 1 mL/min.

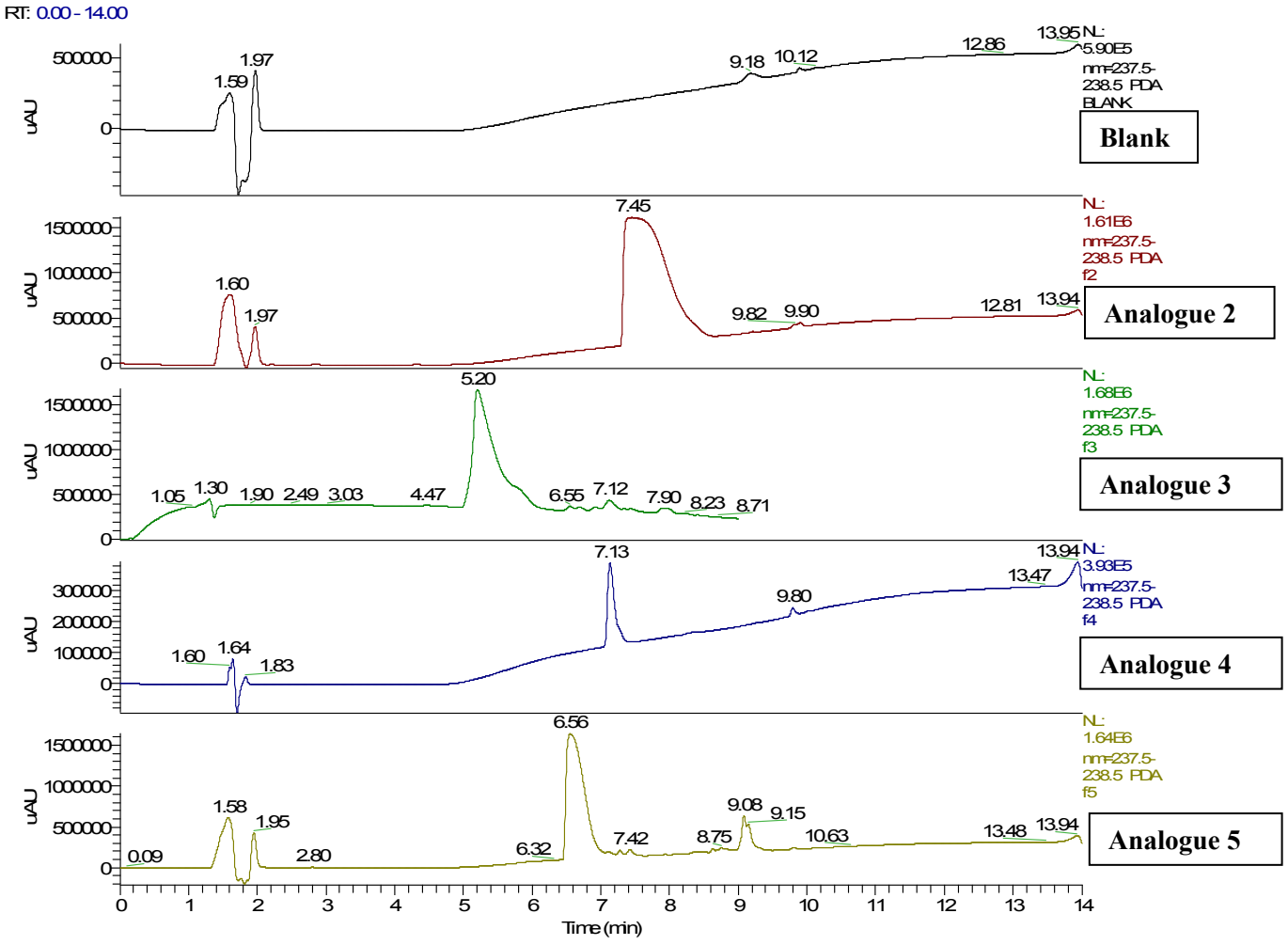

S71. HPLC purity determination of gallinamide analogues 6-9

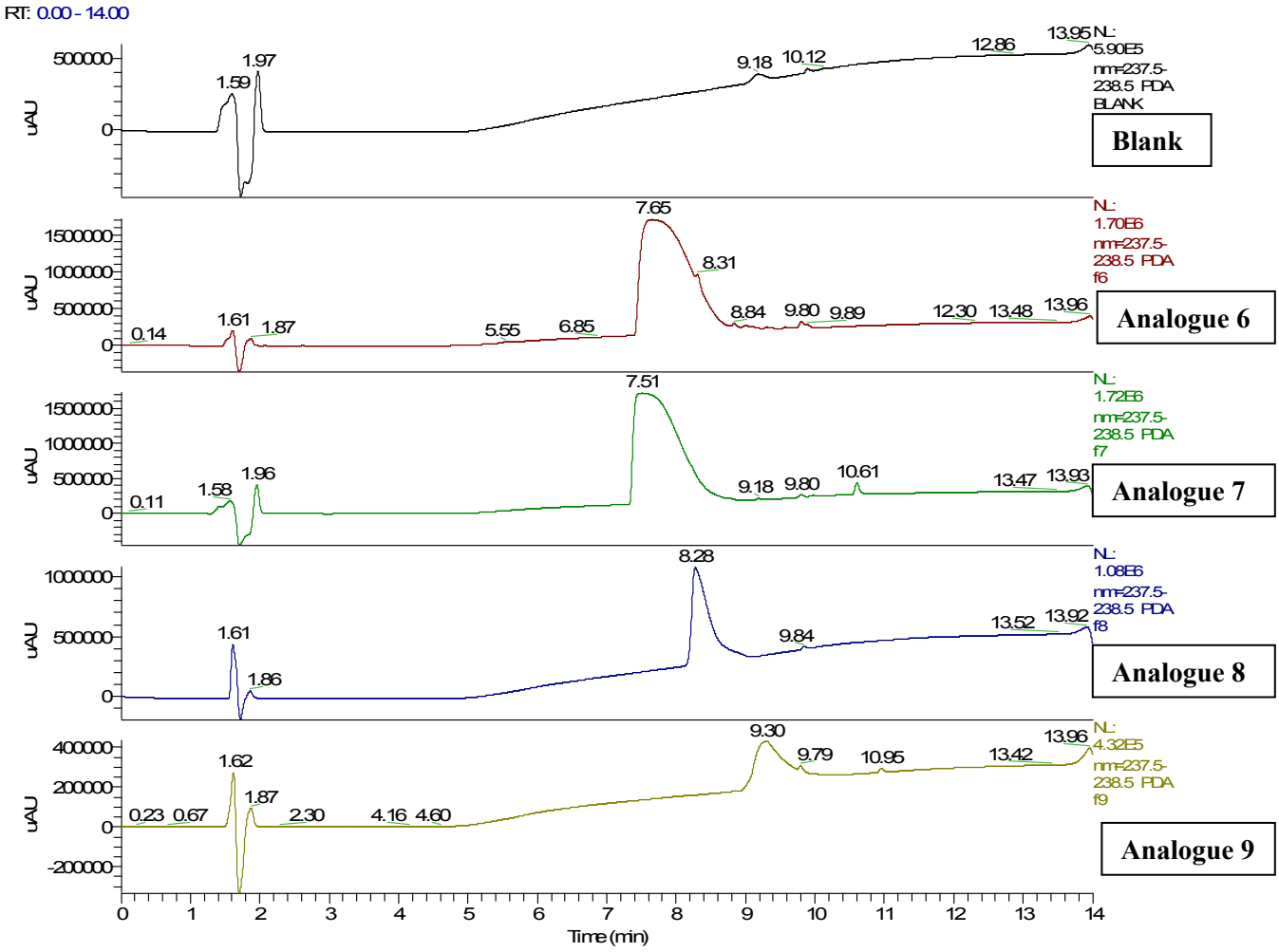

S72. HPLC purity determination for gallinamide analogues 10-13

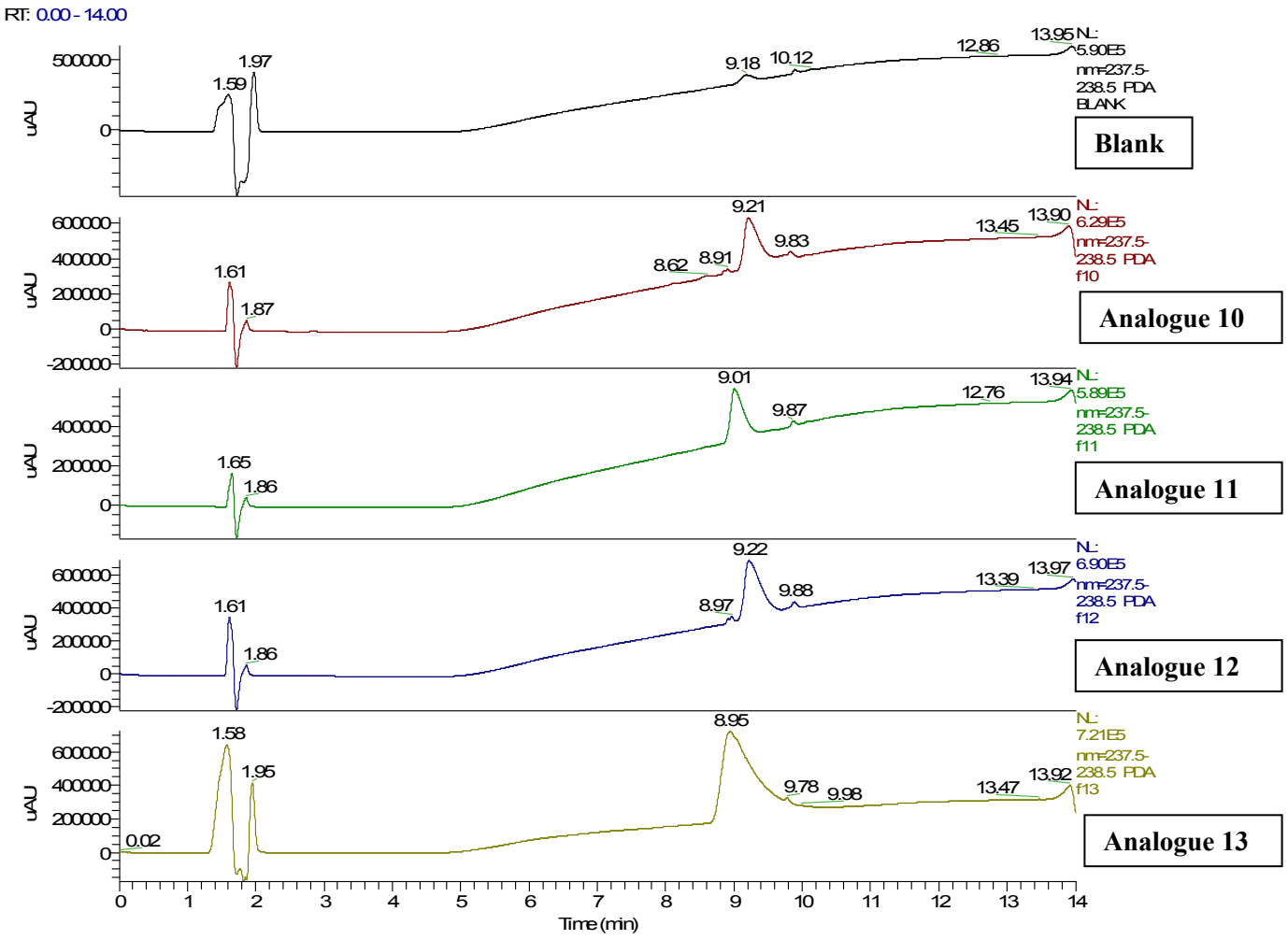

S73. HPLC purity determination for gallinamide analogues 14-17